Calhoun
Institutional Archive of the Naval Postgraduate School

Calhoun: The NPS Institutional Archive

DSpace Repository

Theses and Dissertations | 1. Thesis and Dissertation Collection, all items

1967-12

Comparison of theoretical and experimental stresses in an F8U-3 airplane wing loaded in torsion

Messerschmidt, Donald Bruce

Monterey, California. U.S. Naval Postgraduate School

http://hdl.handle.net/10945/11810

This publication is a work of the U.S. Government as defined in Title 17, United States Code, Section 101. Copyright protection is not available for this work in the United States.

Downloaded from NPS Archive: Calhoun

http://www.nps.edu/library

Calhoun is the Naval Postgraduate School's public access digital repository for research materials and institutional publications created by the NPS community. Calhoun is named for Professor of Mathematics Guy K. Calhoun, NPS's first appointed -- and published -- scholarly author.

Dudley Knox Library / Naval Postgraduate School
411 Dyer Road / 1 University Circle
Monterey, California USA 93943

NPS ARCHIVE
1967
MESSERSCHMIDT, D.

COMPARISON OF THEORETICAL AND EXPERIMENTAL STRESSES IN AN F8U-3 AIRPLANE WING LOADED IN TORSION

DONALD BRUCE MESSERSCHMIDT

COMPARISON OF THEORETICAL AND EXPERIMENTAL STRESSES IN AN F8U-3 AIRPLANE WING LOADED IN TORSION

by

Donald Bruce Messerschmidt

Major, United States Marine Corps

B. S., U. S. Naval Academy, 1959

Submitted in partial fulfillment of the

requirements for the degree of

MASTER OF SCIENCE IN AERONAUTICAL ENGINEERING

from the

NAVAL POSTGRADUATE SCHOOL

December 1967

AFS ARCHIVE
67
DISSERTATION

ABSTRACT

The stresses near the root of an F8U-3 airplane wing loaded in torsion were found using the matrix-force method of analysis. The wing was represented by a simplified, idealized model consisting of axial-load carrying flange bars and shear carrying cover plates. The theoretical stresses in the idealized model were found by using the IBM 360/67 computer to solve for the redundant loads. These stresses show favorable comparison with the experimental stresses determined from strain gages mounted on the cover skin of the wing. This study shows that the matrix-force method is applicable to thick-skinned wings.

NAVAL POSTGRADUATE SCHOOL
MONTEREY CA 93943-5101

TABLE OF CONTENTS

	PAGE
List of Tables	5
List of Illustrations	7
Table of Symbols	9
Introduction	11
Theoretical Analysis	16
Experimental Results	37
Discussion of Results	42
Conclusions	45
References	59
Appendix A: Program Energy	60
Appendix B: Program Recrose	65

LIST OF TABLES

TABLES		PAGE
I	Geometry of Idealized Model	47
II	Geometry of Idealized Model	48
III	The Edge Shear Forces on the Panels	49
IV	Matrix A	50
V	Matrix B	51
VI	Matrix F	52
VII	Matrix P	53
VIII	Experimental Results at Y = 34.5	54
IX	Comparison of Results at Y = 35.5	55
X	Comparison of Theoretical Results at Y = 34.5	56
XI	Matrix of all Internal Loads, with Center Section Included	57
XII	Matrix of all Internal Loads, with Center Section not Included	58

LIST OF ILLUSTRATIONS

FIGURE		PAGE
1.	F8U-3 Wing Center Section	12
2.	F8U-3 Wing Center Section Planform Geometry and Member Location	14
3.	Geometry of Cut at W.S. 25.095	19
4.	Geometry of Cut at W.S. 81.98	20
5.	Geometry of Cut at W.S. 0	21
6.	Exploded View of Outer Section	22
7.	Exploded View of End Rib	23
8.	Determinate Beam	18
9.	Cross Section of Determinate System	24
10.	Flange Bar	27
11.	Force Diagram of Flange Bar	29
12.	Force Diagram of Beam Web	30
13.	Force Diagram of Cover Panel	31
14.	Sweep Coupling of Cover Panel	32
15.	Wing Mounted on Loading Jig	38
16.	Wing with Cover Skin Removed	39
17.	Junction Panel and Budd/Datran Digital Strain Indicator	41

TABLE OF SYMBOLS

$[A]$	Matrix of coefficients of non-redundant loads
$[A]^{-1}$	Inverse of $[A]$ matrix
a_r	Redundant load (pounds)
A.I.B.	Aft intermediate beam
a_{nr}	Non-redundant load (pounds)
$\{AT\}$	Matrix of resultant loads
$[B]$	Matrix of coefficients of redundant and applied loads
$[C]$	Matrix of deflection influence coefficients
C.I.B.	Center intermediate beam
$[CJ]$	$[J]$ matrix designated for computer program
$[E]$	Modulus of elasticity, (psi)
$[F]$	Matrix of flexibility influence coefficients
F.B.	Front Beam
F.I.B.	Forward intermediate beam
FR.I.B.	Front Intermediate beam
$[G]$	$[J]$ matrix augmented by trivial relations
G	Shear modulus, (psi)
$[H]$	Strain energy matrix
$[J]$	Matrix formed by product $[A]^{-1}[B]$
L	Spanwise length, (inches)
P	Applied force, (pounds)
$\{P\}$	Column matrix of applied loads
q	Generalized end loads, (pounds)
R.B.	Rear beam
R.I.B.	Rear intermediate beam
$[S]$	Stress coefficient matrix

T	Torque, (inch - pounds)
t	Thickness (inches)
U	Internal strain energy (inch - pounds)
$[UC]$	C matrix designated for computer program
W	Panel edge length (inches)
W.S.	Wing Station
X_w	X-axis coordinate of wing, (inches)
Y_w	Y-axis coordinate of wing, (inches)
ϵ	Strain, (micro - inches per inch)
μ	Poisson's ratio
σ	Normal stress (psi)
τ	Shear stress (Psi)
ϕ	Angle of principal axis, measured from load reference axis, the C.I.B.
λ	Angle of sweep
$[\ ]$	Rectangular matrix
$\lfloor\ \rfloor$	Row matrix
$\{\ \}$	Column matrix

INTRODUCTION

The purpose of this study is to predict the stresses in an F8U-3 airplane wing loaded in torsion using the matrix-force method of analysis. The stresses determined analytically are compared with the stresses obtained experimentally in order to determine the accuracy and consistency of the results.

The primary structure of the F8U-3 wing center section consists of a simple multicell torque box, as shown in Figure 1. Spanwise bending is carried by the relatively thick skins which are fabricated from 7079-T6 aluminum alloy plate. The skins are machined to varying thicknesses both spanwise and chordwise in order to obtain an optimum distribution of material. The skins are continuous from the wing fold rib inboard to the wing centerline and from the front beam to the rear beam. It is this area, between wing fold ribs, port and starboard, and Front and Rear Beams, fore and aft, which defines the wing center section, the area of interest in this study. The sweep of the wing is 42° at the quarter chord. The wing thickness varies from 4% at the tip to 5.01% at the root. It is this combination of a high degree of sweep and low thickness ratio which raises problems with structural analysis of the wing. Due to bending-torsion interaction, or sweep-coupling, structural analysis by engineering beam theory methods runs into difficulty when analyzing stresses near the wing root.

This thesis describes the matrix-force method of analysis for determining the stress distribution in such a wing. Among the advantages of this method are:

(1) It results in a consistent set of internal stresses and external deflections.

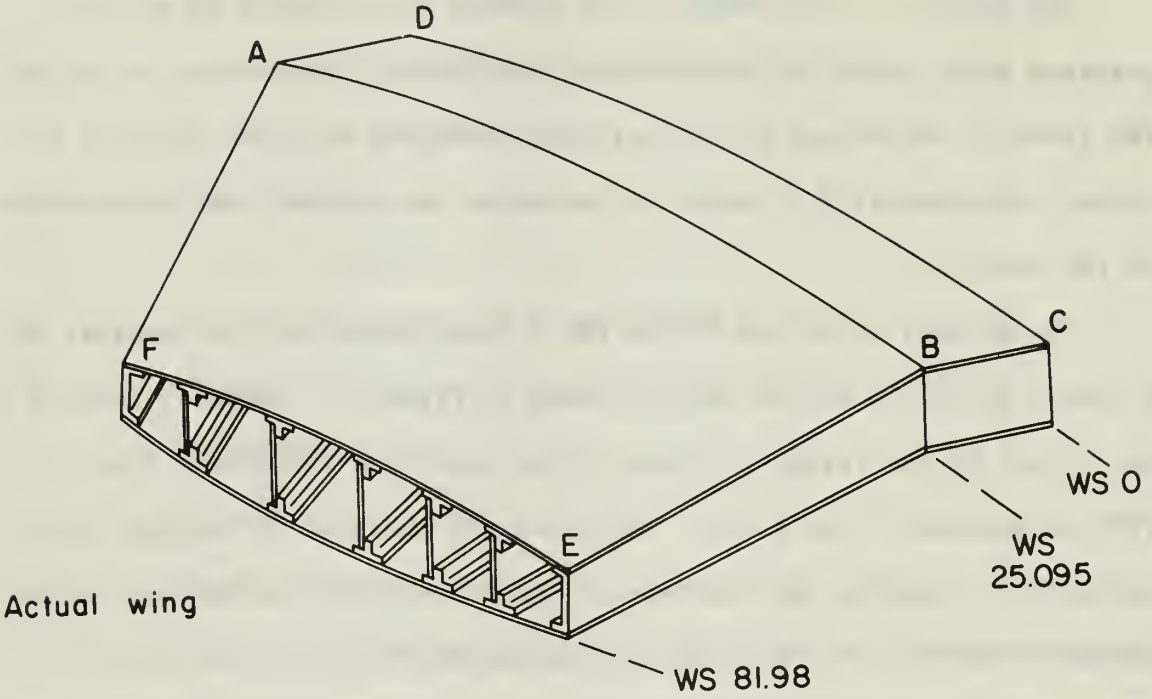

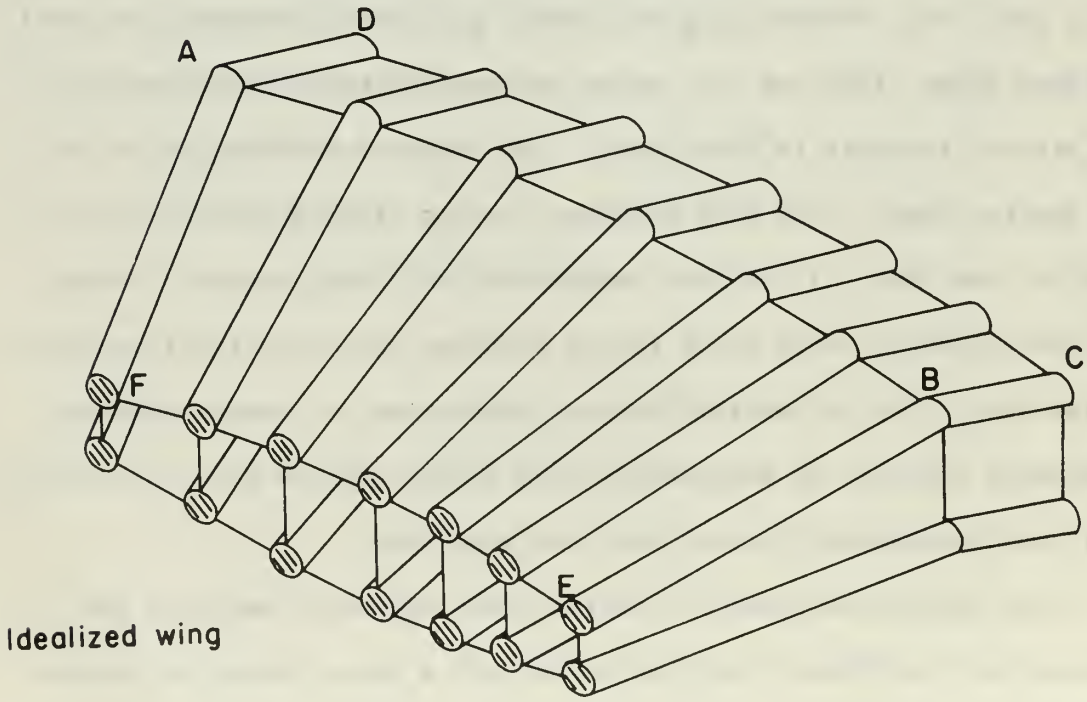

FIG. 1
F8U-3 WING CENTER SECTION

(2) The structure can be altered and re-analyzed with only minor changes in the computer data cards.

(3) The "Bookkeeping" can be simplified and organized in a logical manner.

The matrix-force method of analysis uses forces as the unknowns and treats the structure as an assembly of elastic components. The method, as described in Reference 1, is divided into three parts:

A. Idealize the structure

1. Replace the actual structure with a mathematical model.
2. Make the model statically determinate by cutting redundant members.
3. Write the equilibrium equations that determine the load distribution in the structure

B. Calculate and tabulate the flexibilities of the individual members comprising the structure.

C. Perform matrix operations.

In this report, the wing is "cut" outboard of the intermediate rib (Y_w = 81.98), and it is assumed that the stress distribution here can be accurately calculated using the engineering theory of torsion, $T = \Sigma 2Aq$. The dihedral of the wing is neglected, and the wing is assumed to be supported on four rigid supports located at A, B, C, and D in Figure 2. The aft supports are pins which can support fore and aft and vertical loads. The forward supports can support vertical loads only. The only loading condition considered in this study is symmetrical wing torsion. From symmetry, the reactions at all four support points are determined by equilibrium as functions of the applied loads.

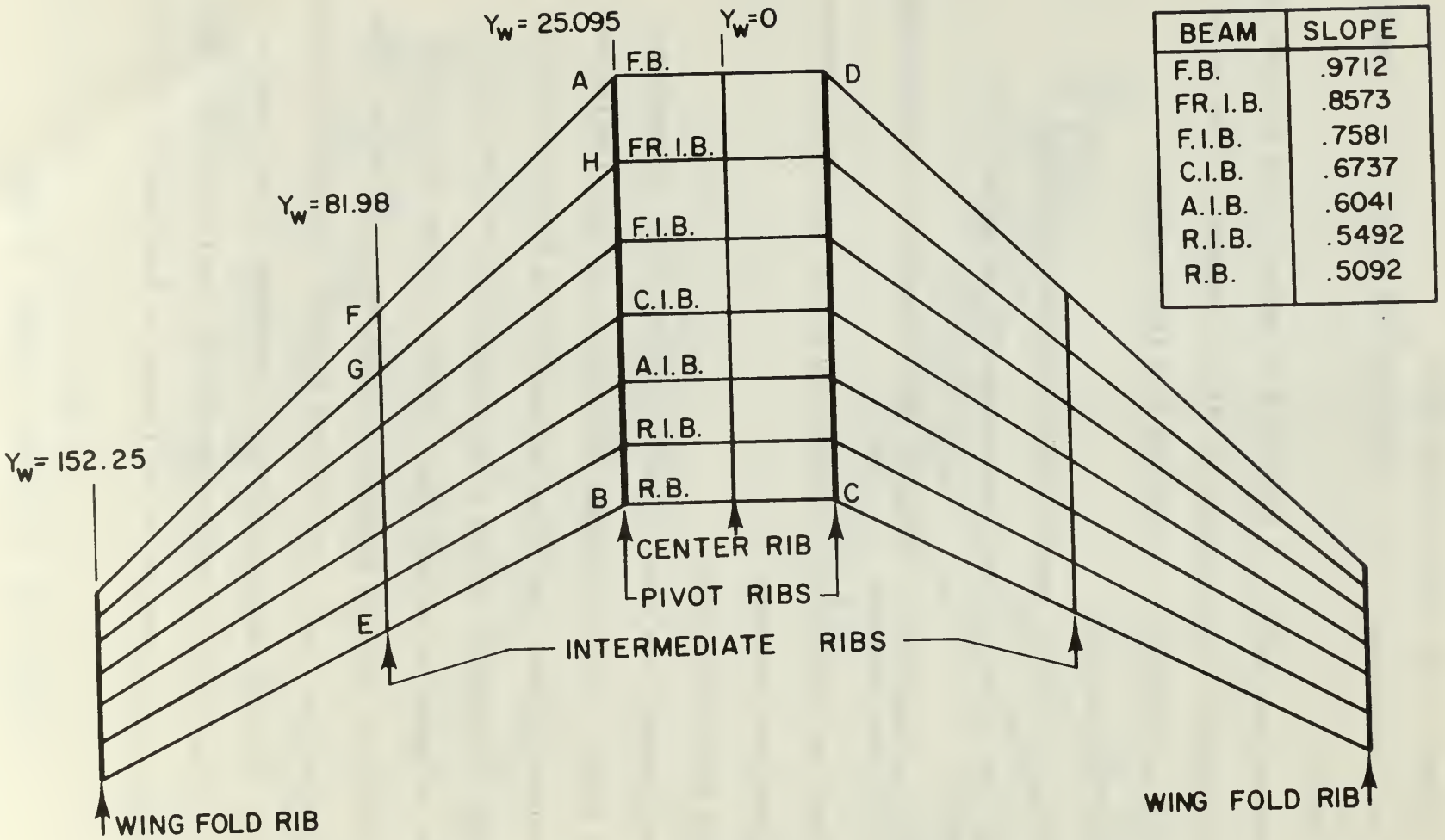

BEAM	SLOPE
F.B.	.9712
FR. I.B.	.8573
F.I.B.	.7581
C.I.B.	.6737
A.I.B.	.6041
R.I.B.	.5492
R.B.	.5092

FIG. 2
F8U-3 WING CENTER SECTION
PLANFORM GEOMETRY & MEMBER LOCATION

This study was conducted at the Naval Postraduate School, Monterey, California, during 1967. The author is indebted to Professor C. H. Kahr who conceived the need for the investigation and who rendered valuable assistance and encouragement throughout the project. The author expresses gratitude to Aeronautical Laboratory Technicians R. A. Besel and T. B. Dunton whose assistance and cooperation were essential to the completion of the study.

THEORETICAL ANALYSIS

A. Idealize the Structure

1. Replace the [illegible] structure with a mathematical model.

The start[illegible] study was a thesis written by [illegible] A. [illegible]olgren and [illegible] [illegible]. This thesis, hereafter referred to as Reference [illegible] [illegible] the wing pivot rib at wing station Y_{W} = [illegible]5.005 did not [illegible] could be used as the effective wing root. The results [illegible] Reference [illegible] showed good correlation between the theoretically predicted [illegible] experimentally [illegible] stresses at the trailing edge [illegible] the [illegible] very poor correlation [illegible] the leading edge. The pivot rib [illegible] in the chordwise direction since its web and flanges are [illegible] to the wing beam[illegible] especially near the wing [illegible] [illegible]9.8, the upper flange is .88 in. thick, the lower flange [illegible] in. thick and the web [illegible] in. thick.) The cross section [illegible] resembles an "I" beam which is known to have low [illegible] about its longitudinal axis. [illegible] decided that the pivot rib [illegible] compared to the wing beams, [illegible] through to the [illegible] ABCD of Figure [illegible]. [illegible] with the previously [illegible] to correct for [illegible] of the pivot rib. [illegible] the [illegible] divided [illegible] as shown in Figure [illegible]. [illegible] this rib [illegible] the [illegible] and the [illegible] the [illegible]

The model selected to represent the wing structure consisted of flat plates which carry only shear and cylindrical bars which carry only axial load. This model was selected for compatibility with the previous work done in Reference 2. Analysis of the model can be as accurate as the matrix-force method and arithmetic permit; however, the correlation between theoretical and experimental stresses will depend upon how closely the model represents the actual structure. This study is not an attempt to define the best model for the analysis, but to calculate stresses in what was tacitly assumed to be an adequate model. Most of the examples of similar studies currently available in the literature deal with thin-skinned shells. There is little evidence on whether or not such models are suitable for the thick-skinned wing plates used in this study. An important factor in constructing the idealized model is the change of the wing geometry to model geometry. The model consists of bars and flat shear carrying plates. It is extremely important to insure that these plates are, in fact, mathematically flat. For example, the depths of the ribs at WS 25.095 and WS 81.98 were such that the four points AFGH in Figure 1 did not lie in a plane. Therefore,panel AFGH is warped and has panel edge shears which have components perpendicular to plane AFGH. These shears are not accounted for in the equilibrium equations written for a flat panel and will produce errors in the solution. Reference 3 shows that for a similar wing such discrepancies yielded determinate member loads which were out of equilibrium as much as 5 to 10%. After altering the beam depths to make the panels flat, this trouble disappeared. The alteration required a change of less than 1% of each dimension.

After determining model geometry from the adjusted dimensions of the wing, the cross sectional area of the bars and the thickness of the shear panels were calculated. Each bar area of the model consists of the area of the beam flange plus one half the skin area between adjacent beams. The beam web areas were not included, using the methods of Reference 4. The effect of combining the axial load carrying skin with the beam flange to form the model's cylindrical bar is to remove Poisson's effect from the analysis. This means that any chordwise contraction of the cover skins is neglected. The wing skin thickness varies in the chordwise direction in section ABCD and in both spanwise and chordwise directions in section ABEF. An average skin thickness between beams was determined and used as the shear plate thickness. Using constant thickness shear plates in place of tapered skin simplifies the analysis but introduces possible sources of error. Model geometry and areas are listed in Tables I and II. Diagrams of cross sectional geometry are shown in Figure 3, 4, and 5. An exploded view of the outer section of the idealized model from Y_w = 25.095 to Y_w = 81.98 is shown in Figure 6. An exploded view of the intermediate rib at Y_w = 81.98 is shown in Figure 7.

2. Make the model statically determinate by cutting redundant members.

The most complex beam that is truly determinate, so that the flange and shear loads can be determined from equilibrium equations, is the 3-flange, 3 web beam shown in Figure 8.

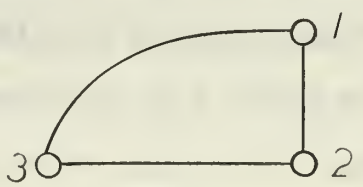

Fig 8.

DETERMINATE BEAM

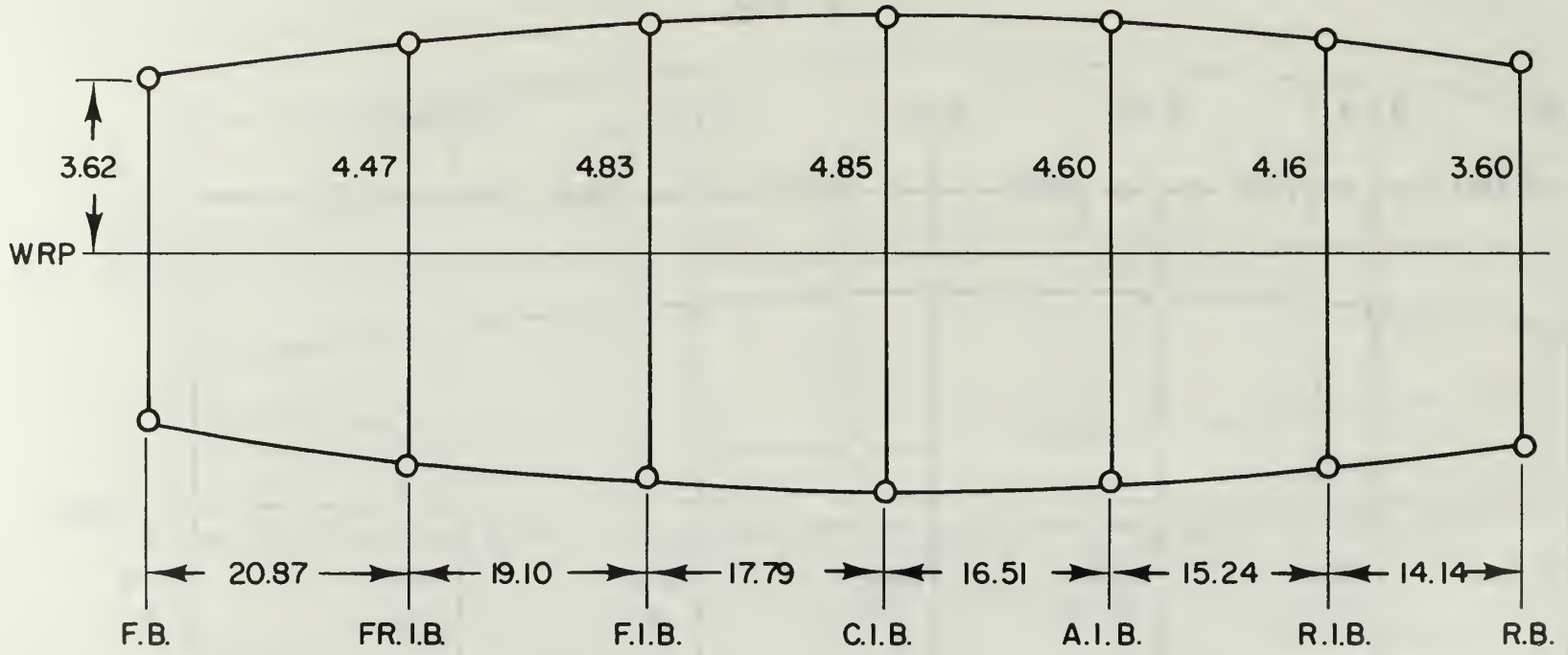

FIG. 3
F8U-3 WING CENTER SECTION
GEOMETRY OF CUT AT W.S. 25.095

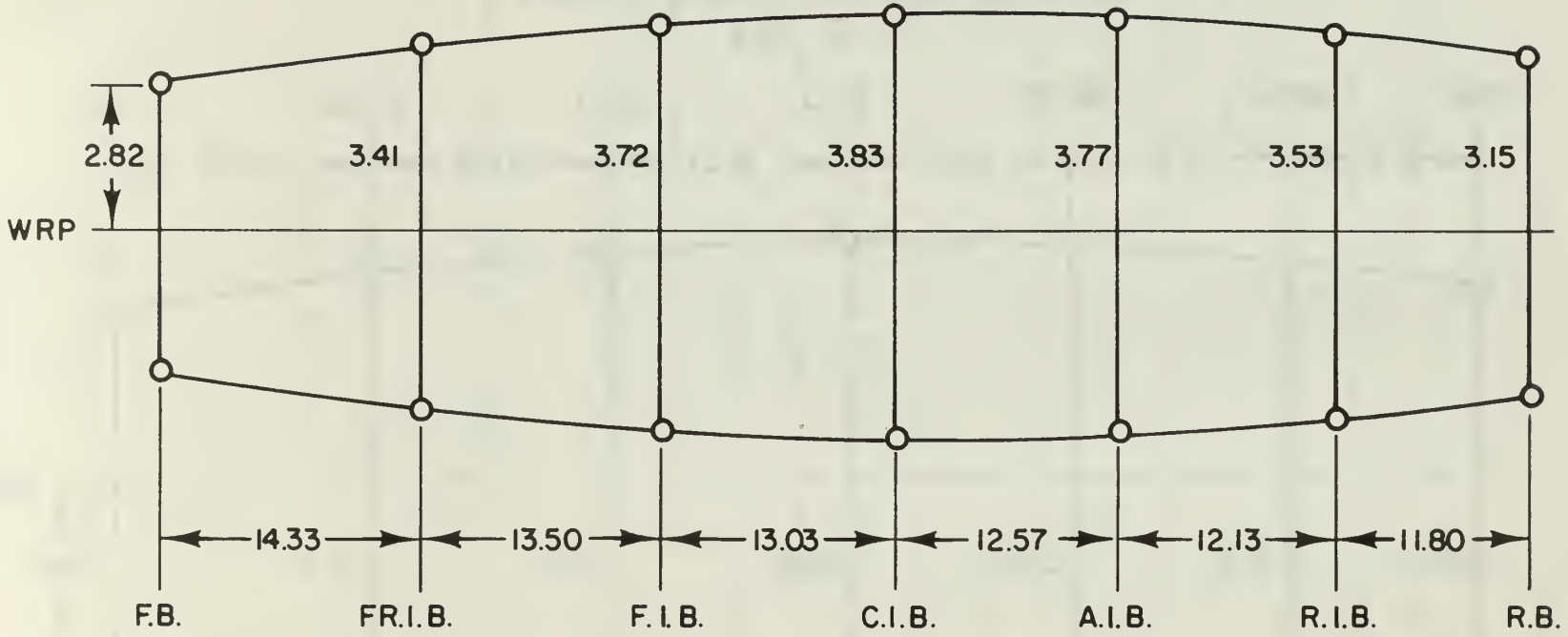

FIG. 4
F8U-3 WING CENTER SECTION
GEOMETRY OF CUT AT W.S. 81.98

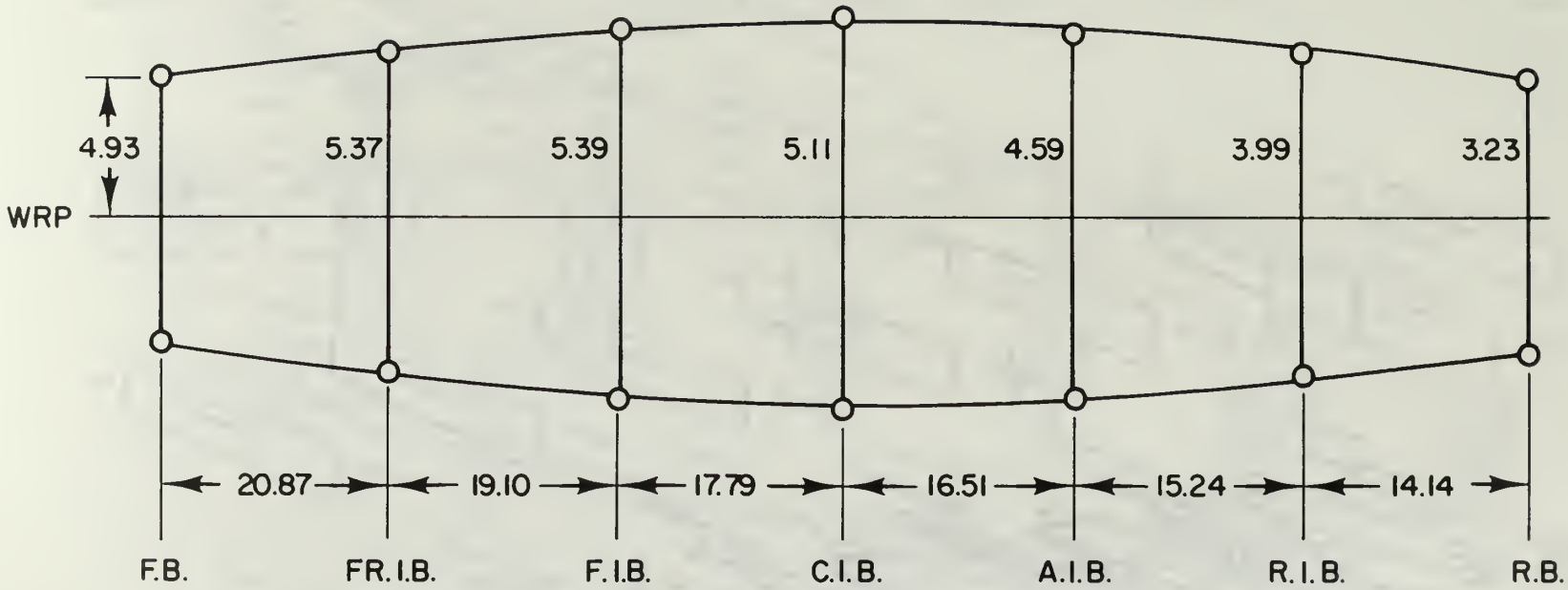

FIG. 5
F8U-3 WING CENTER SECTION
GEOMETRY OF CUT AT ℄ RIB (Y=0)

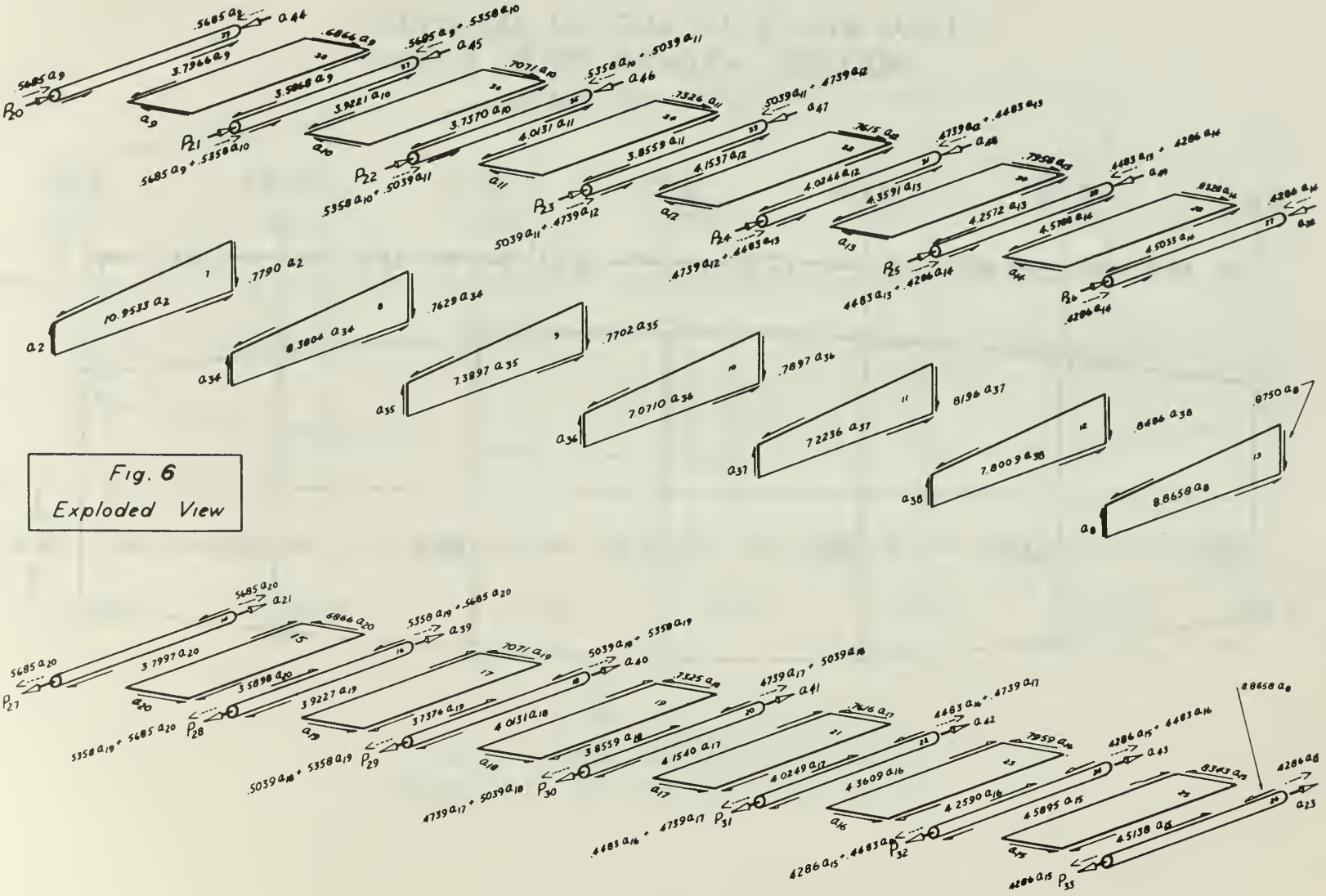

Fig. 6
Exploded View

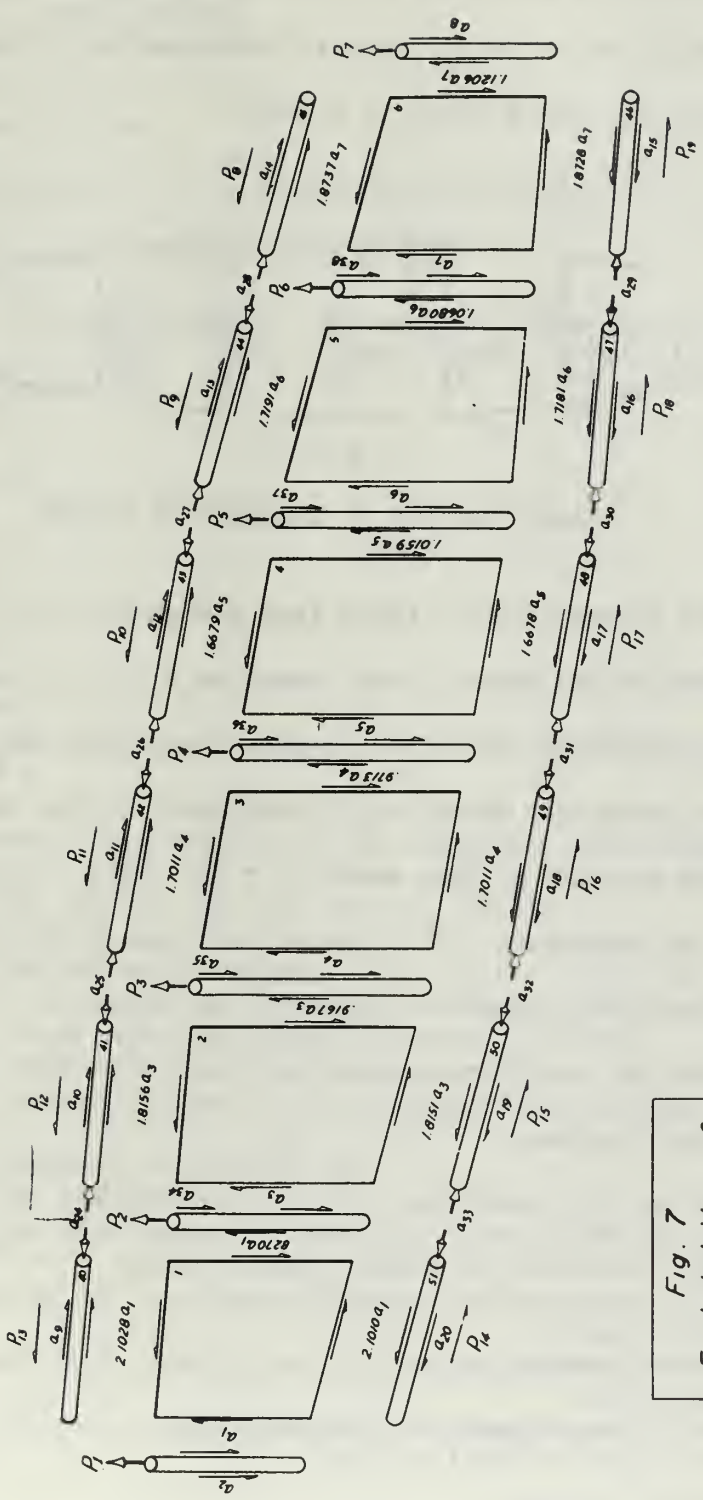

Fig. 7
Exploded View of
End Rib

In this beam, loads can be obtained from equilibrium only, without considering flange areas, material stiffness, or deformation of the structure. In order to make the idealized model of this study a determinate structure, it was necessary to cut the 5 interior webs and 11 of the flanges, resulting in the structure shown in Figure 9.

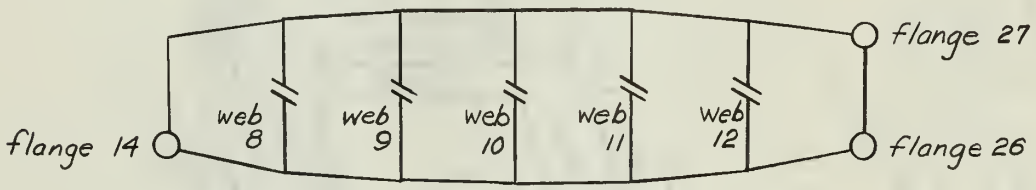

Fig. 9

CROSS SECTION OF DETERMINATE SYSTEM

The number of redundancies arising from the geometry of a box structure has been given by Reference 4 and others as B + N - 4 where B is the number of longitudinal effective flanges continuous across each junction and N is the number of closed cells stiffened by ribs at tip end of bay. For the outer section of this model, B = 14 and N = 6, which results in 16 degrees of redundancy. This agrees with the 16 members which were cut to provide the determinate structure of Figure 7.

3. Write the equilibrium equations that determine the load distribution in the structure.

Considering the outer wing section from station 25.095 to 81.98, there are the following 49 unknown member loads.

12	skin panels
14	beam flanges
7	beam webs
10	rib flange loads at station 81.98
6	rib webs at station 81.98
49	total unknowns

The redundant forces come from the following members.

1	F.B. ,	upper flange
2	FR.I.B.,	both flanges
2	F.I.B. ,	both flanges
2	C.I.B. ,	both flanges
2	A.I.B. ,	both flanges
2	R.I.B. ,	both flanges
5	webs 8 - 12	
16	redundant forces	

Thus, there are 49 - 16 or 33 equations of equilibrium required to characterize the model. These equations are:

a) Six equations of equilibrium of free body of bay between stations Y_w = 25.095 and 81.98

(1) $P_x = 0$

(2) $P_y = 0$

(3) $P_z = 0$

(4) $M_{xx} = 0$

(5) $M_{yy} = 0$

(6) $M_{zz} = 0$

b) Eleven equations of equilibrium of the redundant beam flanges, elements 16, 18, 20, 22, 24, 29, 31, 33, 35, 37, and 39.

c) Ten equations of forces and moments, $F_x = 0$, $M_{yy} = 0$ of the intermediate beam segments of the rib at Y_w = 81.98

d) Six equations of equilibrium of the rib posts on the beam ends at Y_w = 81.98, elements 53 through 58.

The addition of the center section Y_w = 0 to 25.095 can be thought of as an extention of the horizontal flanges. The forces in the X and Z directions are reacted by the horizontal and vertical supports at Y_w = 25.095, but the Y forces carry through to the centerline, Y_w = 0.

Although the center section is 16° redundant (the same as the outboard section), these are not new redundancies but merely components of the forces in the outer section. Further investigation shows that for symmetrical wing loading, the bending meoment, M_x, is constant from $Y_w = 25.095$ to $Y_w = 25.095$ and that torsional and vertical shear are zero. The axial load on each flange at $Y_w = 25.095$ is the same as the load on each flange at $Y_w = 25.095$. Hence there is no shear on any panel or web in the center section. (It was later shown that due to a slightly unsymmetrical load, there are, in fact, shearing stresses in the center section panels.) Since the addition of the center section results in no new redundancies and no new external loads, there can be no more than the 33 independent equilibrium equations already proposed for the outer section. Since there are more than 33 structural elements involved, there are several possible combinations of 33 independent equations. Those chosen were considered to be those most likely to have the larger stress concentrations.

B. Calculate and tabulate the flexibilities of the individual members comprising the structure.

As described in Section C, the internal strain energy of the wing may be written as:

$$2EU = \lfloor a_1\ a_2 \cdots a_{49} \rfloor \, [F]_{49\times 49} \begin{Bmatrix} a_1 \\ a_2 \\ \vdots \\ a_{49} \end{Bmatrix} \qquad (1)$$

The elements in the F matrix define the elasticity of the structure. If skin thicknesses or flange areas are changed, only the elements of the F matrix will be affected. If the geometry of the model is changed, the equations of equilibrium will also be affected. Multiplying out equation 1,

$$2EU = a_1^2 F_{11} + a_2^2 F_{22} + \cdots a_n^2 F_{nn} + 2a_1 a_2 F_{12} + 2a_1 a_3 F_{13} + \cdots \quad (2)$$

Each term of Equation 2 can be regarded as a small increment of strain energy ΔU associated with the load a_i^2 or $a_i \cdot a_j$. Since the load a_i may be applied to more than one structural element, the corresponding F_{ii} term may be made up of contributions from several structural elements. The F matrix must be a square symmetric matrix where $F_{ij} = F_{ji}$.

1. Flange Bars.

The calculation of the F matrix elements for the flanges was done following the example of Reference 4. The energy in a uniform bar under a linearly varying axial force is

$$U = \frac{1}{2AE}\int_0^\ell \left[q_1 + \frac{q_2 - q_1}{L}\,x\right]^2 dx \quad (3)$$

where q_1 and q_2 are end forces as shown in Figure 10.

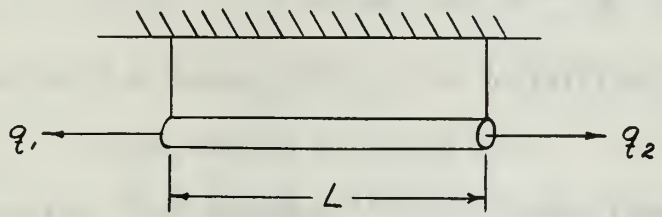

Fig. 10

FLANGE BAR

Rewriting Equation 2 for this single element

$$2EU = q_1^2 f_{11} + 2q_1 q_2 f_{12} + q_2^2 f_{22} \quad (4)$$

therefore

$$f_{11} = E\frac{\partial^2 U}{\partial q_1^2} = \frac{1}{A}\int_0^\ell \frac{x}{L}\left(1 - \frac{x}{L}\right) dx \quad (5)$$

$$f_{11} = \frac{L}{3A} = f_{22} \quad (6)$$

and $$f_{12} = f_{21} = E\frac{\partial^2 U}{\partial q_1 \partial q_2} = \frac{1}{A}\int_0^{\ell} \frac{x}{L}\left(1 - \frac{x}{L}\right)dx$$

$$f_{12} = f_{21} = \frac{L}{6A} \tag{7}$$

In the case of linearly tapered members, the flexibilities may be obtained as functions of the end area ratios. Reference 1 shows the flexibility influence coefficients modified by a function, Q, of the end areas which was obtained from a graph of Q versus A_i / A_j, the end area ratio.

$$f_{11} = \frac{L}{3A}\Phi_{11}\ , \quad f_{12} = \frac{L}{6A}\Phi_{12}\ , \quad f_{22} = \frac{L}{3A}\Phi_{22} \tag{8}$$

For most of the flange elements, the generalized end loads, q_i and q_j were linear functions of the unkown member loads, or:

$$q_i = \alpha_1 a_1 + \alpha_2 a_2 + \cdots \alpha_n a_n \tag{9}$$

$$q_j = \beta_1 a_1 + \beta_2 a_2 + \cdots \beta_n a_n \tag{10}$$

where α_i = the coefficient of the i'th member load applied to one end of the bar,

and β_i = the coefficient of the i'th member load applied to the other end of the bar.

Now taking each force acting on the ends of the flange individually, that is:

$$q_1 = \alpha_1 a_1 \tag{11}$$

$$q_2 = \beta_1 a_1 \tag{12}$$

and substituting into Equation 4, we find that

$$2EU = a_1^2(\alpha_1 f_{11} + 2\alpha_1\beta_1 f_{12} + \beta_1^2 f_{22}) \tag{13}$$

and from Equation 1, for a single force, a_1

$$2EU = a_1^2 F_{11} \tag{14}$$

Comparing Equations 13 and 14,

$$F_{11} = \alpha_1^2 f_{11} + 2\alpha_1\beta_1 f_{12} + \beta_1^2 f_{22} \tag{15}$$

Similarly, for the other forces acting on the same flange,

$$F_{22} = \alpha_2^2 f_{11} + 2\alpha_2\beta_2 f_{12} + \beta_2^2 f_{22} \tag{16}$$

and for the cross product term,

$$F_{12} = \alpha_1\alpha_2 f_{11} + \beta_1\beta_2 f_{22} + f_{12}(\beta_1\alpha_2 + \beta_2\alpha_1) \tag{17}$$

The forces on element 14 are shown in Figure 11.

For example, the flexibility influence coefficients for element 14 were determined as follows:

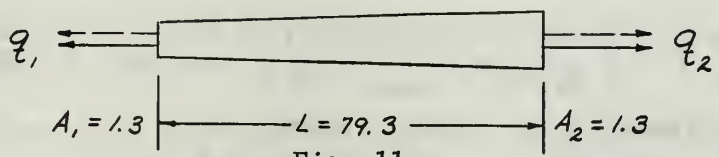

Fig. 11

FORCE DIAGRAM OF FLANGE BAR

$$f_{11} = \frac{L}{3A_1}\Phi_{11} = 20.333 = f_{22}$$

$$f_{12} = \frac{L}{6A_1}\Phi_{12} = 10.167$$

$$q_1 = -3.231\,a_{20} + a_{21} - 10.953\,a_2$$

$$q_2 = .568\,a_{20} + a_{21}$$

$$F_{2,2} = 20.333(-10.953)^2 + 2 \times 10.167(-10.953)(0) + 20.333(0)^2 = 2439.483$$

$$F_{2,20} = 20.333(-3.231)^2 + 20.333(0)(.568) + 10.167(-10.953)(.568) = 656.335$$

For element 14, there are 4 more coefficients to be found; $F_{20,\ 20}$, $F_{21,\ 21}$, $F_{2,\ 21}$, and $F_{20,\ 21}$. The $F_{2,\ 2}$ coefficient for element 14 is added to other $F_{2,\ 2}$ coefficients for elements 7, 39, 101, and 126 to make up the total $F_{2,\ 2}$ flexibility influence coefficent found in the F matrix.

2. Symmetrical Shear Panels

Reference 3 gives the energy of the symmetrical trapezoidal panel in terms of the shear force on the shorter parallel side, as:

$$2EU = \left\{ \frac{\ell_d (W_1 + W_2)}{W_1^2 t} \left[\frac{1}{6} \left(\frac{W_1 - W_2}{\ell_d} \right)^2 + (1+\mu) \right] \right\} a_n^2 \tag{18}$$

so that

$$F_{n,n} = E \frac{\partial^2 U}{\partial a_n^2} \tag{19}$$

may be written for $F_{1,1}$ of element 1

$$F_{1,1} = \left\{ \frac{14.335(12.460)}{46.512(.200)} \left[\frac{1}{6}(.00678) + 1.32 \right] \right\}$$

The forces on element 1 are shown in Figure 12.

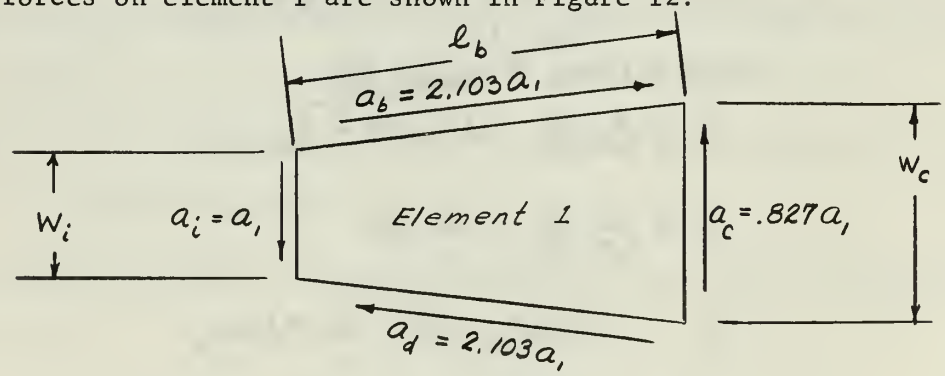

Fig. 12

FORCE DIAGRAM OF BEAM WEB

Other $F_{1,\ 1}$ coefficients appear from elements 40 and 51 and add to produce the final $F_{1,\ 1}$ found in the F Matrix.

The shear panel edge loads were determined by assigning a unit shear force, a_i, to the outboard edge of all panels and the forward edge of the rib webs. From the equilibrium of the free body, forces a_b, a_c, and a_d may be found as functions of the unit force a_i.

$$a_b = a_i \, l_b / W_c$$

$$a_c = a_i \, W_i / W_c \qquad (20)$$

$$a_d = a_i \, l_d / W_c$$

The geometry of the panels and the load ratios are shown in Table III.

3. Non-symmetrical shear panels.

a) The cover skin panels have roughly the shape of a parallelogram, with the inclined sides skewed slightly. The maximum difference in inclination, $\delta - \beta = 3° \; 34'$, occurs at the forward panels, elements 38 and 15. These panels were treated in accordance with Reference 6 which shows that the energy of the swept panel is given as

$$2EU = \left[(1+\mu) \left(\frac{W_1 + W_2}{lt} \right) \sin^2 \delta \left(1 + \frac{2\gamma}{3(1+\mu)} \right) \right] a_4^{\,2} \qquad (21)$$

where $\gamma = \cot^2 \beta + \cot \delta \cot \beta + \cot^2 \delta$ (22)

The forces on element 15 are shown in Figure 13.

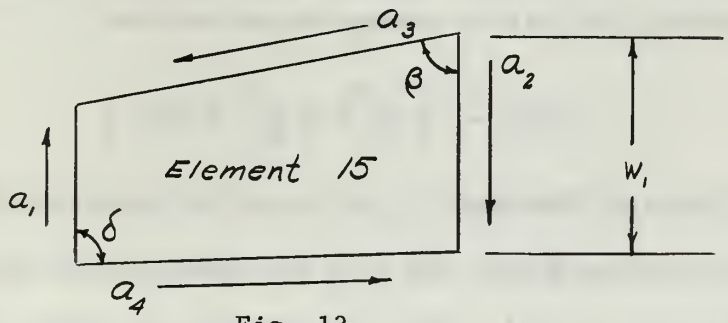

Fig. 13
FORCE DIAGRAM OF COVER PANEL

so that

$$F_{n,n} = E \frac{\partial^2 U}{\partial a_4^{\,2}}$$

may be written for $F_{20,\,20}$ of element 15.

$$F_{20,20} = 1.32 \left(\frac{35.199}{8.647} \right) .576 \left(1 + 1.268 \right) \left(3.590 \right)^2 = 90.525$$

b) The cover skin panels introduce additional forces due to interaction between torsion and bending. Twist of a swept wing produces bending and vice-versa. This interaction was introduced by considering the stress distribution in the rhomboidal cover skin panels, as shown in Figure 12. These panels were assumed to be parallelograms in order to simplify the analysis. Consider the plate shown, loaded with a uniform shear force, a , and axial load, f_t.

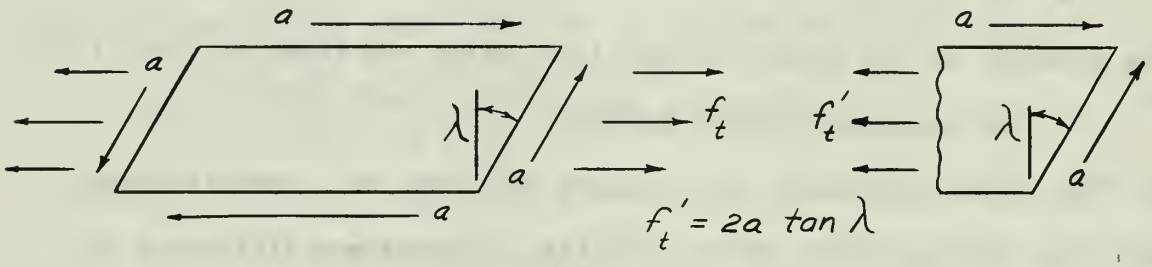

Fig. 14

SWEEP COUPLING OF COVER PANEL

The axial force, f_t, was assumed concentrated at the flanges which were made up mostly of skin material, so that the cover panels carry only shear. However, it is seen in Figure 12 that the shear forces along the sides of the panel produce additional tensile stresses, f_t', which do work on the displacements produced by the primary axial stress, f_t. For this panel, the strain energy can be written.

$$2EU = D f_t^2 + E q^2 + F f_t q \tag{23}$$

The third term in Equation 22 is due to the interaction between the axial and shearing forces and does not appear in an equation written for a rectangular panel. This term causes the stress distribution in this model to show a root stress concentration. Reference 3 states that "Studies made on simple one cell swept box models with streamwise ribs, utilizing parallelogram shaped cover sheets, show that unless this cross-product term is introduced, there will be nothing in the analysis to

differentiate between a straight and swept wing, and there will be no root stress concentration factor"[3]. For the purpose of calculating the energies in the flanges adjacent to each panel, this axial load, f'_t, was split equally and added to the end of each flange. These coupling loads are shown as dashed vectors in Figure 6.

C. Perform matrix operations.

The matrix-force method, as described in References 1 and 3, expresses the energy of the entire structure as the successive product of three matrices.

$$2EU = [a]\,[F]\,\{a\} \tag{24}$$

where a_1 ..... a_n are the internal loads acting on the members. The F matrix is symmetrical and represents the elasticity of the structure. The internal loads were found by writing the equilibrium equations for the determinate structure and for each redundant member. The number of equations must equal the total number of unknown internal loads less the number of redundants. The equations are written so that all the independent external loads and redundants are collected on one side and non-redundant loads on the other side of the equality;

such as

$$[A]\,\{a_{nr}\} = [B]\,\{P \mid a_r\} \tag{25}$$

where $[A]$ and $[B]$ are matrices of the coefficients of the loads. Solving for the non-redundant loads, a_{nr}, as functions of the applied loads, P, and the redundants, a_r, we get:

$$\{a_{nr}\} = [A]^{-1}[B]\,\{P \mid a_r\} = [J]\,\{P \mid a_r\} \tag{26}$$

Then, by adding the trivial relation between the redundants

$$\{a_r\} = \{a_r\} \tag{27}$$

and expanding $[J]$ to include Equation 4 results in

$$\{a\}_{TOTAL} = [G]\{P \mid a_r\} \tag{28}$$

which may be transposed, yielding Equation 6

$$\{a\}^T = \lfloor a \rfloor = \lfloor P \mid a_r \rfloor [G]^T \tag{29}$$

Now, substituting into Equation 1,

$$\begin{aligned} 2EU &= \lfloor P \mid a_r \rfloor G^T F G \{P \mid a_r\} \\ &= \lfloor P \mid a_r \rfloor [H] \{P \mid a_r\} \end{aligned} \tag{30}$$

$[H]$ is a symmetric matrix. Its members are the coefficients of the strain energy terms when the energy is written as a function of applied and redundant loads. Partitioning $[H]$ into four sub-matrices,

$$[H] = \left[\begin{array}{c|c} H_{11}\ p\times p & H_{12}\ p\times r \\ \hline H_{21}\ r\times p & H_{22}\ r\times r \end{array}\right]$$

P = applied loads = 33
r = redundant loads = 16

Rewriting Equation 29,

$$2EU = P^2 H_{11} + 2P a_r H_{12} + a_r^2 H_{22} \tag{31}$$

Minimizing the strain energy with respect to the redundant, a_r, yields

$$\frac{\partial U}{\partial a_r} = 0 = 2PH_{12} + 2a_r H_{22} \tag{32}$$

Rearranging

$$\begin{aligned} \{a_r\} &= -[H_{22}]^{-1}[H_{21}]\{P\} \\ &= [EN]\{P\} \end{aligned} \tag{33}$$

The matrix of all the unknown internal loads is given by

$$\{a\}_{TOTAL} = [G]\left[\frac{I_{p\times p}}{EN_{r\times p}}\right]\{P\} \tag{34}$$

$$\{a\}_{TOTAL} = [S]\{P\}$$

S is the unit load distribution matrix for the indeterminate structure. Each S_{im} term is the value of the i'th member load when the structure is subjected to a unit value of the m'th applied load.

Using the notation of Reference 5, the strain energy can be written:

$$U = \frac{1}{2}\{P\}[C]\{P\} \tag{35}$$

where C is the matrix of flexibility influence coefficients. Substituting from Equation 11 into Equation 23,

$$U = \frac{1}{2E}\left[\{P\}[S]^T[F][S]\{P\}\right] \tag{36}$$

therefore

$$C = \frac{1}{E}[S]^T[F][S] \tag{37}$$

$$= \frac{1}{E}\left[I \mid EN\right] G^T F G \left[\frac{I}{EN}\right]$$

$$= \frac{1}{E}[EN][H][EN]$$

and substituting $EN = -[H_{22}]^{-1}[H_{21}]$ from Equation 10,

$$C = \frac{1}{E}\left([H_{11}] - [H_{12}][H_{22}]^{-1}[H_{21}]\right) \tag{38}$$

Note that Equation 34 may be expanded to read

$$a_1 = s_{11} P_1 + s_{12} P_2 \cdots s_{1m} P_m \tag{39}$$

$$a_2 = s_{21} P_1 + s_{22} P_2 \cdots s_{2m} P_m$$

Therefore, each internal load, a_i , may be found by substituting a particular set of applied loads, $\{P\}$. For any other loading condition, only the matrix of applied loads needs to be changed to obtain the new internal loads for that loading (flight) condition. This enables a rapid evaluation of the maximum load on any element over a range of applied loads.

A computer program, originally set up by Reference 2 for the CDC 1604 computer was rewritten in Fortran IV to fit the IBM 360/67 computer and appears in Appendix A. This program performs the complete matrix operation outlined in Section C with input A and B from the flexibility matrix and the applied loads, P. Matrices A, B, F, and P appear in Tables IV, V, VI, and VII.

In order to ascertain whether or not the results obtained from the strain energy method were accurate for this type of thick skinned wing construction, it was necessary to have experimental data with which to compare the results of the idealized model. The wing is mounted in a jig which closely approximates the actual method of joining the wing to the aircraft fuselage, as shown in Figure 15. Since the wing is a continuous structure, the root fixity coefficient is not changed as when a single span wing is mounted on a completely rigid bulkhead. The loading condition investigated was a torque of 336,000 in. lbs. This load was considered to be well within the elastic range, but still of sufficient magnitude to give adequate strain levels throughout the structure for repeatable strain measurements. Some strain gages were installed on the wing when received from Ling-Temco-Vought Aerospace Corp., and others were installed at the Naval Postgraduate School. Figure 16 shows the wing with one cover skin removed for installation of strain gages. Wing section $Y_w = 34.5$ was particularly well instrumented, with strain gage rosettes placed on both sides of top and bottom skins to check for differential bending effects. Strain gage data were reduced to principal stresses and directions through computer program "Recrose", written in Fortran IV for the IBM 360/67 computer, as shown in Appendix B. The torque loads were applied with four hydraulic cylinders through a heavy fitting attached to the wing fold lugs. The applied torque was designed to be perpendicular to the elastic axis. The load was applied at both wing fold axes; and to ensure a symmetrical load, the four hydraulic cylinders were supplied through a common manifold.

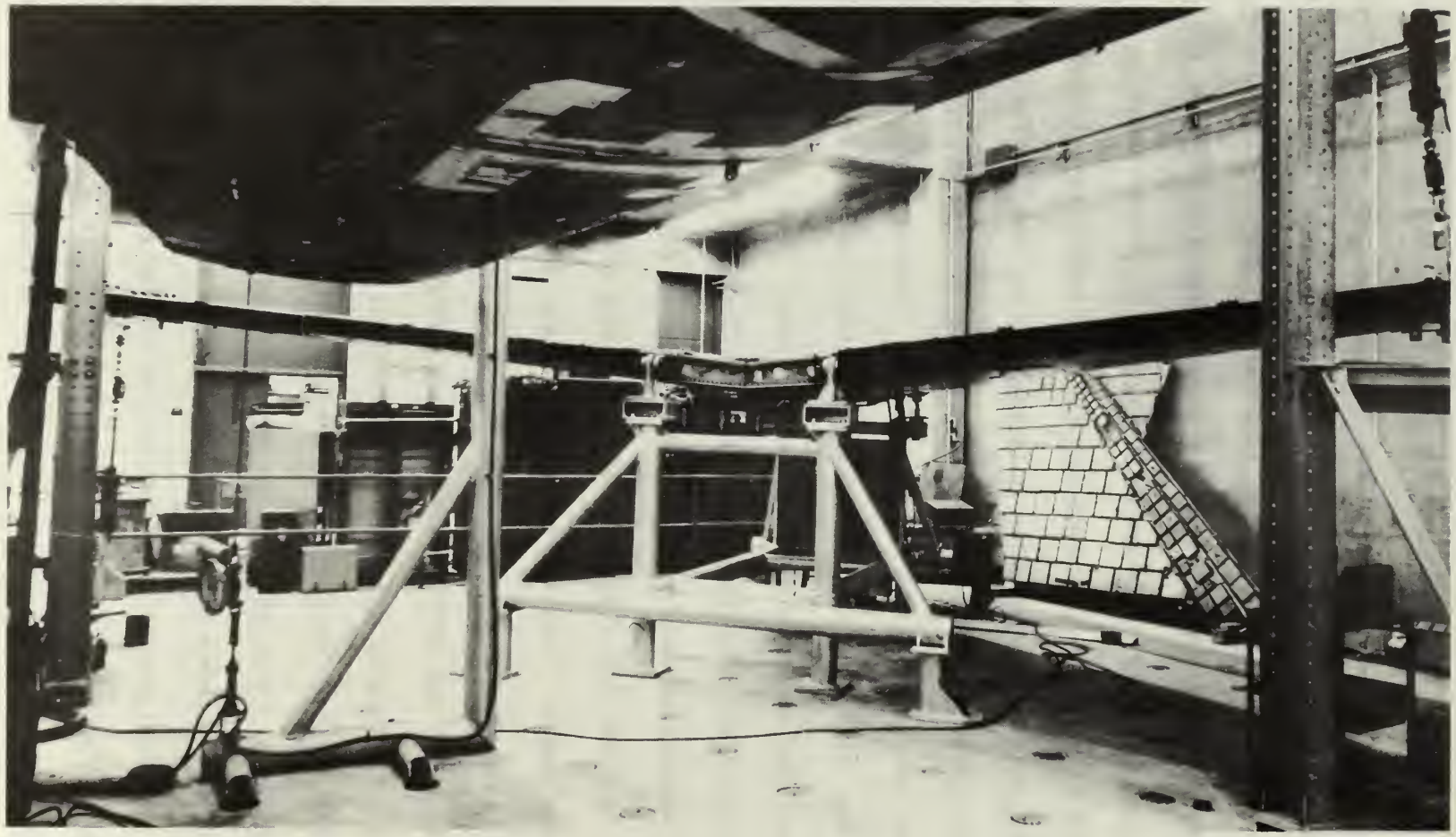

FIG. 15
Wing Mounted on Loading Jig

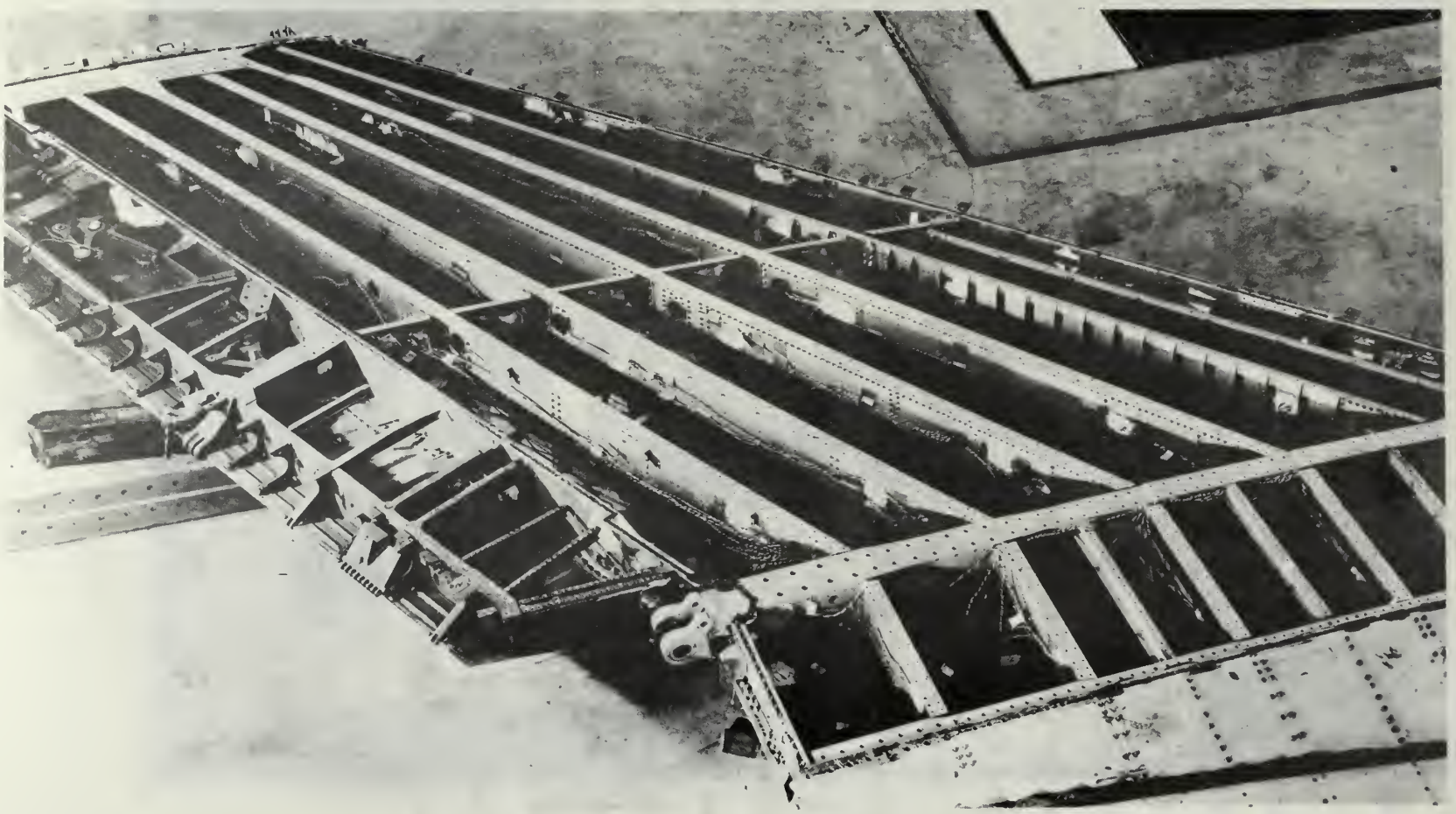

FIG. 16

Wing with Cover Skin Removed

Load magnitude was determined by a manifold pressure gage in the hydraulic pressure system and checked by four Dillon dynamometers attached to each cylinder. The strain readings were taken with a Budd/Datran digital strain indicator (Model TC22). All gages were wired to a common junction panel as shown in Figure 17. All gages were balanced at a zero reading before applying the load. Eighteen gages were read at each loading in about one minute. This minimized the chance for drift in gage reading. All gages were rechecked for their zero reading after the load was released and sufficient time had elapsed for hysteresis effects to be minimized. All testing was done at night to eliminate the thermal effects of sunlight shining on the wing. Reference 2 contains all strain gage coordinates, gage factors and resistances. It also shows that the strains are in the linear region by comparing the gage readings at a loading of 8000 psi (336,000 in. lbs. of torque) with those taken at 7000 psi (294,000 in. lbs. of torque) and extrapolated to 8000 psi.

Strain readings for the rosettes on the cover panels appear in Table VIII. The readings were averaged for the back-to-back gages and entered in program "Recrose" to compute the stresses. The normal and shearing stresses and the principal axes for the skin panels are also shown in Table VIII.

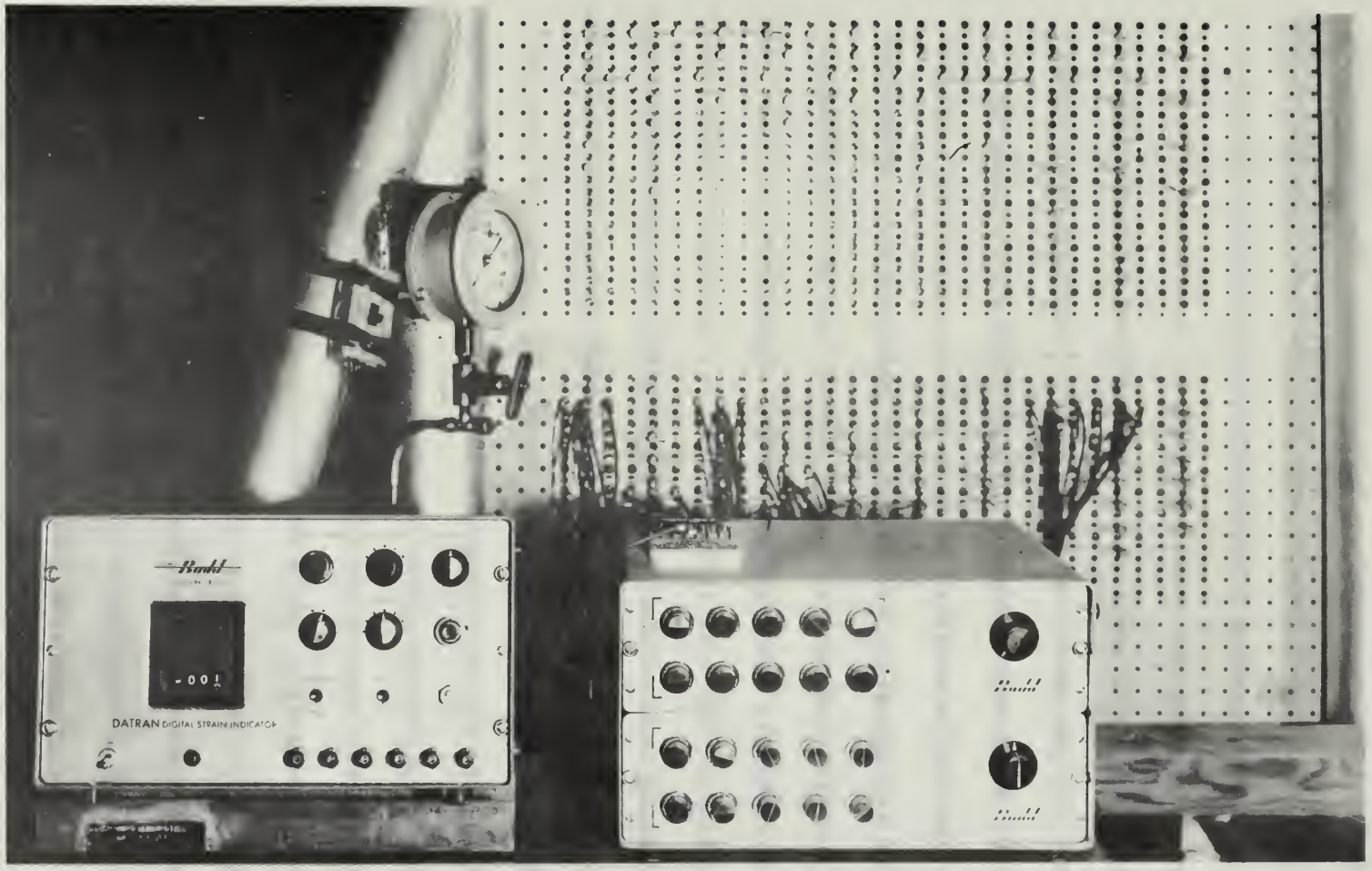

FIG. 1?

Junction Panel and Budd / Datran Digital Strain Indicator

There are two areas of comparison in this study. The first is the comparison of the theoretical results with the experimental results, and the second is the comparison of the theoretical analysis of the wing with and without including the center section.

In the first area, the stresses as found in Table IX show fairly close agreement. In the panels where the best stress agreement occurs, such as panel 38, the strain readings on both sides of the skin are nearly equal. The strain readings of back-to-back gages were averaged and used to find the experimental stresses at each station. Where the corresponding interior and exterior gages showed considerable variance in their strain readings, the experimental and theoretical stresses also had greater variance. The difference in strain readings is due to differential bending in the cover skin and possible torsional resistance of the pivot rib at the rear fitting, both of which were neglected in the theoretical analysis. The differential bending was neglected because the model used for the flexibility coefficient of the cover skin was a flat panel which carries only shear. The torsional resistance of the pivot rib was neglected because the effect of an unknown amount of slack movement about the wing hinge could not be incorporated into the theoretical analysis. The strain gages themselves are believed to be accurate to within 5 micro-inches of the true strain values. Strain readings found by Holgren and Comfort in 1963 were very close to those found in this study. The substitution of aluminum pads between the jig and the loading floor for the original plywood pads, as recommended in Reference 2, does not seem to have made much difference in the strain

values. The original gages were carefully installed and waterproofed which seems to account for their longevity. Most of the gages have been in place for over four years. The normal expected life-span of this type gage in industrial use is one or two years. The first factor mentioned, that of differential bending and torsional resistance of the pivot rib, seems most likely to be the cause of the difference between theoretical and experimental results. The differences do not seem to be too great since some of the references mention that errors of 100% are sometimes found in the case of thin skinned structures. More conclusive comparisons could be made if the torque loading were increased and larger strain readings were available. However, it was decided that a significant increase in the torque loading beyond the 336,000 in. lbs. used in this study might permanently warp the wing and render it useless for further study.

The second area of comparison is between the theoretical results found in this study, and those of Reference 2. Including the center section, from $Y_w = 0$ to $Y_w = 25.095$ resulted in changing 25 flexibility influence coefficients and did not change the equilibrium equations. In effect, it moved the wing root from the pivot rib at $Y_w = 25.095$ to the center rib at $Y_w = 0$. Most of the coefficients changed by 3 or 4%, and none of them changed by more than 13%; yet the matrix of resultant loads, $\{AT\}$, shows some considerable changes. In comparing $\{AT\}$ of Reference 2 with the $\{AT\}$ matrix found in this study, the former loads will be designated as a_j (Reference 2). The greatest change was in the load on the rear intermediate beam, R.I.B. a_j (Reference 2) = 1010.4; and $a_{43} = 10,263.5$. This load is applied to element 24 and will influence the stresses on panels 23 and 25. The flexibility coefficient associated

with this force has a much smaller change, $F_{43,\ 43}$ (Ref. 2) = 13.3832 and $F_{43,\ 43}$ = 14.3406. The purpose of mentioning these changes is to show that the cumulative effect of minor changes in 25 out of 129 non-zero flexibility coefficients may be great. This means that small errors in deciding upon the true area and length of the elements of the idealized model may be significant. When the actual structure to be idealized has irregular cut-outs and joints, and reduction in skin, web, and flange areas occurs in steps rather than linearly, considerable effort will be involved in just constructing an idealized model. By examining Table X, it is seen that inclusion of the center section relieved the stresses at the leading edge of the wing which was the area of greatest discrepancy in Reference 2. Both normal and shear stresses are much closer to the experimental values. The stresses in the rear panels are also improved, but it is felt that the pins at point B and C in Figure 2 fit snugly enough to offer some torsional resistance of the pivot rib at the rear fitting, which was not accounted for in the theoretical analysis. Tables XI and XII list the resultant loads, a_1 through a_{49} for the wing with and without center section included. The agreement between theoretical and experimental stresses throughout the wing seems to bear out the validity of the matrix-force method, and the approach as described in this study in the prediction of stresses in a wing prior to its construction. For greater accuracy, it would be necessary to use more elements which would require the calculation of additional equilibrium equations and hence expansion of the matrices.

The matrix-force method of analysis using the strain energy theory, as proposed in Reference 1, is acceptable for a thick-skinned wing. It can be expected to predict the stresses in a complex, highly redundant structure, loaded in torsion, with a reasonable degree of accuracy. For increased accuracy, the long slender panels representing the cover skin should be broken up, and smaller elements used which would reduce the size of the structural grid but increase the number of unknowns. Reference 7 mentions a method of accomplishing this by dividing each panel into a number of narrow longitudinal strips which could be treated as rectangles with constant shear flow in each one. The difference in shear forces of adjacent strips would be taken by assuming concentrated stringer areas in the spanwise direction. This method would still neglect Poisson's effect. From the results of this study, it appears that a better panel would be one whose length and width were of similar size.

In summation, it was found that the accuracy of the matrix-force method was improved considerably (compared with the results found in Reference 2) by the inclusion of 14 additional members which resulted in changes to 25 flexibility coefficients. Generally speaking, it must be possible to attain a very high degree of accuracy by fundamentally the same method as has been used in this study, by dividing the structure into a much larger number of elements. This involves a larger number of redundancies and much more numerical work. This could be programmed to be accomplished by the computer. An experienced stress analyst, who knows the stress distribution of most of the elements of the structure

on which he is working, would be able to concentrate the redundancies to the unknown points, thus reducing the computational work considerably. The experimental analysis would be improved by the addition of more strain gages on the inside of the wind cover skins.

Because of the number of man - hours involved in removing and replacing the cover skins, however, it would not be practical to install additional gages.

BEAM	LENGTH	AVG. WEB THICK-NESS	Station Y_w = 25.095						Station Y_w = 81.98					
			UPPER SKIN EFF. AREA	UPPER FLANGE EFF. AREA	EQUIV. UPPER FLANGE	LOWER SKIN EFF. AREA	LOWER FLANGE EFF. AREA	EQUIV LOWER FLANGE	UPPER SKIN EFF. AREA	UPPER FLANGE EFF. AREA	EQUIV UPPER FLANGE	LOWER SKIN EFF. AREA	LOWER FLANGE EFF. AREA	EQUIV. LOWER FLANGE
OUTBOARD SECTION Y_w = 25.095 to Y_w = 81.98														
FB	79.302	.162	.974	.364	1.50*	.824	.304	1.30*	1.13	.364	1.50	1.00	.304	1.30*
FRIB	74.921	.032	2.840	.203	3.04	2.390	.134	2.52	2.48	.203	2.68	2.14	.134	2.27
FIB	71.385	.040	4.800	.370	5.17	3.720	.134	3.85	3.06	.370	3.43	2.69	.134	2.82
CIB	68.589	.063	6.510	.370	6.88	4.950	.134	5.08	3.50	.370	3.87	3.18	.134	3.31
AIB	66.457	.063	7.640	.370	8.01	6.080	.134	6.21	3.50	.370	3.87	3.17	.134	3.30
RIB	64.904	.090	7.990	.370	8.36	6.690	.134	6.82	3.47	.370	3.84	3.15	.134	3.28
RB	63.834	.200	3.920	.206	4.13	3.410	.206	3.62	1.74	.206	1.95	1.58	.206	1.79
CENTER SECTION STATION Y_w = 0 to 25.095														
FB	25.095	0	1.356	.364	1.882*	1.148	.304	1.614*						
FRIB	25.095	0	2.931	.203	3.134	2.341	.134	2.475						
FIB	25.095	0	3.931	.370	4.275	2.968	.134	3.102	* includes .162 for post beam.					
CIB	25.095	0	5.261	.370	5.631	3.570	.134	3.704						
AIB	25.095	0	6.451	.370	6.821	5.290	.134	5.424						
RIB	25.095	0	7.166	.370	7.536	5.939	.134	6.073						
RB	25.095	0	3.646	.206	3.852	3.044	.206	3.250						

TABLE I

Geometry of Idealized Model

PANEL (from L.E.)	AVG. SKIN THICKNESS		END WIDTH		AVG. SWEEP ANGLE	END RIB Y_w = 81.98			
	UPPER	LOWER	Y_w = 25.095	Y_w = 81.98		BAR	EFF. WEB AREA	EFF. COVER SKIN AREA	EFF. BAR AREA
1	.175	.152	20.88	14.34	42°23'	40	.28	3.02	3.30
2	.250	.211	19.10	13.51	38°53'	41	.28	4.06	4.34
3	.370	.300	17.79	13.03	35°34'	42	.28	4.32	4.60
4	.420	.350	16.51	12.58	32°33'	43	.28	4.72	5.00
5	.477	.400	15.24	12.13	29°57'	44	.28	4.54	4.82
6	.490	.420	14.16	11.81	27°53'	45	.28	4.42	4.70
						46	.28	3.84	4.12
						47	.28	3.88	4.16
						48	.28	3.78	4.06
						49	.28	3.94	4.22
						50	.28	4.06	4.34
						51	.28	2.58	2.86

TABLE II

Geometry of Idealized Model

TABLE III

THE EDGE SHEAR FORCES ON THE PANELS

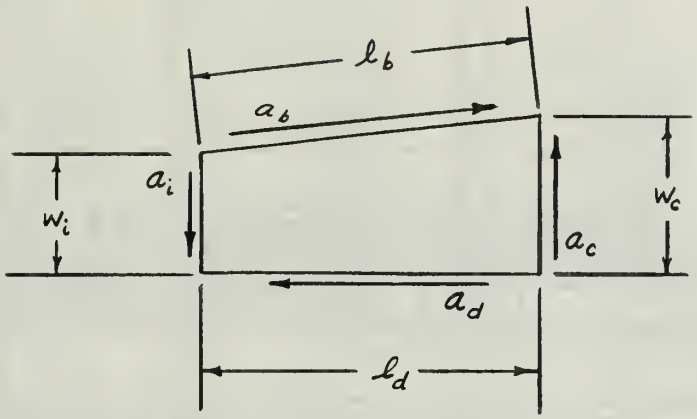

Piece No.	w_i in.	w_c in.	l_b in.	l_d in.	$a_b/a_i = l_b/w_c$	$a_c/a_i = w_i/w_c$	$a_d/a_i = l_d/w_c$
1	5.64	6.82	14.3408	14.3287	2.1027	.8269	2.1009
2	6.82	7.44	13.5077	13.5041	1.8155	.9166	1.8150
3	7.44	7.66	13.0307	13.0303	1.7011	.9712	1.7010
4	7.66	7.54	12.5756	12.5754	1.6678	1.0159	1.6678
5	7.54	7.06	12.1370	12.1296	1.7191	1.0679	1.7180
6	7.06	6.30	11.8046	11.7984	1.8737	1.1206	1.8727
7	5.64	7.24	79.3021	79.3021	10.9533	.7790	10.9533
8	6.82	8.94	74.9206	74.9206	8.3803	.7628	8.3803
9	7.44	9.66	71.3846	71.3846	7.3897	.7701	7.3897
10	7.66	9.70	68.5890	68.5890	7.0710	.7896	7.0710
11	7.54	9.20	66.4567	66.4567	7.2235	.8195	7.2235
12	7.06	8.32	64.9038	64.9038	7.8009	.8485	7.8009
13	6.30	7.20	63.8339	63.8339	8.8658	.8750	8.8658
15	14.3287	20.8705	79.3021	74.9206	3.7997	.6865	3.5897
17	13.5041	19.0991	74.9206	71.3846	3.9227	.7070	3.7375
19	13.0303	17.7879	71.3846	68.5890	4.0130	.7325	3.8559
21	12.5754	16.5114	68.5890	66.4567	4.1540	.7616	4.0249
23	12.1296	15.2393	66.4567	64.9038	4.3608	.7959	4.2589
25	11.7984	14.1418	64.9038	63.8339	4.5894	.8342	4.5138
28	11.8046	14.1748	64.9038	63.8339	4.5788	.8327	4.5033
30	12.1320	15.2456	66.4567	64.9038	4.3590	.7957	4.2571
32	12.5756	16.5132	68.5890	66.4567	4.1535	.7615	4.0244
34	13.0307	17.7879	71.3846	68.5890	4.0130	.7325	3.8559
36	13.5077	19.1022	74.9206	71.3846	3.9220	.7071	3.7369
38	14.3408	20.8878	79.3021	74.9206	3.7965	.6865	3.5868

TABLE IV

MATRIX A INPUT FORM

1 1	1.0	1 2	1.0	124	0.0	133	0.0	1
2 2	-10.95333	2 9	-3.79656	3 3	0.91667	3 4	-1.0	1
325	0.01451	332	-0.01451	4 4	0.97128	4 5	-1.0	1
426	0.01321	431	-0.01321	5 5	1.01592	5 6	-1.0	1
527	0.01502	530	-0.01502	6 6	1.06799	6 7	-1.0	1
628	0.01242	629	-0.01242	7 7	1.12064	7 8	-1.0	1
8 8	90.69401	8 9	2.48330	810	2.88222	811	3.50534	1
812	4.35896	813	5.36467	814	6.40125	815	6.40751	1
816	5.36585	817	4.35940	818	3.50521	819	2.88194	1
820	2.48326	821	2.52213	822	2.31101	823	2.31101	1
9 9	3.58680	910	-3.92209	1010	3.73698	1011	-4.01309	1
1111	3.85592	1112	-4.15356	1212	4.02444	1213	-4.35905	1
1313	4.25719	1314	-4.57881	14 7	13.2218	1414	7.0563	1
1428	7.05861	1515	4.58948	1516	-4.25897	1616	4.36087	1
1617	-4.02490	1717	4.15404	1718	-3.85593	1818	4.01309	1
1819	-3.73758	1919	3.92272	1920	-3.58977	20 9	-0.68600	1
2010	-0.70702	2011	-0.73256	2012	-0.76146	2013	-0.79544	1
2014	-0.83085	2015	0.83235	2016	0.79561	2017	0.76154	1
2018	0.73254	2019	0.70694	2020	0.68598	2021	0.69672	1
2022	-0.45372	2023	0.45372	2121	0.71728	2122	-0.89112	1
2123	0.89112	2221	2.59655	2222	3.20803	2223	3.20803	1
2322	-92.3649	2323	92.3649	24 3	12.37883	2410	6.81821	1
2424	6.81426	2425	-6.81821	25 4	12.65607	2511	7.43973	1
2525	7.43802	2526	-7.43973	26 5	12.77567	2612	7.65992	1
2626	7.65969	2627	-7.65992	27 6	12.95433	2713	7.53852	1
2727	7.53991	2728	-7.53852	2814	1.0	2815	-1.0	1
2828	1.00032	2829	1.00032	29 2	0.77901	29 8	0.87500	1
29 9	-0.02794	2910	- 0.01333	2911	- 0.00820	2912	0.01153	1
2913	0.02297	2914	0.03290	2915	0.03296	2916	0.02297	1
2917	0.01153	2918	- 0.00082	2919	- 0.01333	2920	- 0.02794	1
2921	0.01009	2922	0.00654	2923	0.00654	3013	1.0	1
3016	-1.0	3027	1.00019	3028	-1.0	3029	-1.0	1
3030	1.00019	3112	1.0	3117	-1.0	3126	0.99997	1
3127	-1.0	3130	-1.0	3131	0.99997	3211	1.0	1
3218	-1.0	3225	0.99977	3226	-1.0	3231	-1.0	1
3232	0.99977	3310	1.0	3319	-1.0	3324	0.99942	1
3325	-1.0	3332	-1.0	3333	0.99942			2

TABLE V
MATRIX B INPUT FORM

1 1	1.0	134	0.0	220	1.0	244	-1.0	1
3 3	-1.0	335	1.0	4 4	-1.0	436	1.0	1
5 5	-1.0	537	1.0	6 6	-1.0	638	1.0	1
7 7	-1.0	8 1	55.2466	8 2	69.5754	8 3	83.0796	1
8 4	96.1099	8 5	108.6853	8 6	120.8150	8 7	132.6135	1
8 8	7.4179	8 9	5.9191	810	4.2884	811	3.0187	1
812	1.8124	813	0.5448	814	0.5448	815	1.8124	1
816	3.0187	817	4.2884	818	5.9191	819	7.4172	1
820	2.5220	821	3.2013	822	3.5384	823	3.5707	1
824	3.3099	825	2.8758	826	2.3642	827	2.5220	1
828	3.2013	829	3.5384	830	3.5707	831	3.3099	1
832	2.8758	833	2.3642	834	-15.9213	835	-30.7843	1
836	-45.6107	837	-60.8687	838	-75.9532	839	-3.2013	1
840	-3.5384	841	-3.5707	842	-3.3099	843	-2.8758	1
844	-2.5220	845	-3.2013	846	-3.5384	847	-3.5707	1
848	-3.3099	849	-2.8758	921	1.0	934	8.3804	1
945	-1.0	1022	1.0	1035	7.3897	1046	-1.0	1
1123	1.0	1136	7.0710	1147	-1.0	1224	1.0	1
1237	7.2236	1248	-1.0	1325	1.0	1338	7.8009	1
1349	-1.0	14 7	0.0	14 8	7.0563	1532	-1.0	1
1538	-7.8009	1543	1.0	1631	-1.0	1637	-7.2236	1
1642	1.0	1730	-1.0	1736	-7.0710	1741	1.0	1
1829	-1.0	1835	-7.3897	1840	1.0	1928	-1.0	1
1934	-8.3804	1939	1.0	20 8	-0.99948	20 9	-0.99980	1
2010	-0.99999	2011	-0.99996	2012	-0.99974	2013	-0.99915	1
2014	0.99915	2015	0.99974	2016	0.99996	2017	0.99999	1
2018	0.99980	2019	0.99948	2020	-0.69666	2021	-0.65009	1
2022	-0.60391	2023	-0.55916	2024	-0.51788	2025	-0.48235	1
2026	-0.45373	2027	0.69666	2028	0.65009	2029	0.60391	1
2030	0.55916	2031	0.51788	2032	0.48235	2033	0.45373	1
2039	-0.65009	2040	-0.60391	2041	-0.55916	2042	-0.51788	1
2043	-0.48235	2044	0.69666	2045	0.65009	2046	0.60391	1
2047	0.55916	2048	0.51788	2049	0.48235	2120	-0.71732	1
2121	-0.75927	2122	-0.79688	2123	-0.82936	2124	-0.85597	1
2125	-0.87645	2126	-0.89114	2127	0.71732	2128	0.75927	1
2129	0.79688	2130	0.82936	2131	0.85597	2132	0.87645	1
2133	0.89114	2139	-0.75927	2140	-0.79688	2141	-0.82936	1
2142	-0.85597	2143	-0.87645	2144	0.71732	2145	0.75927	1
2146	0.79688	2147	0.82936	2148	0.85597	2149	0.87645	1
22 1	56.885	22 2	56.885	22 3	56.885	22 4	56.885	1
22 5	56.885	22 6	56.885	22 7	56.885	22 8	1.83113	1
22 9	1.12519	2210	0.27134	2211	-0.48011	2212	-1.30551	1
2213	-2.34025	2214	-2.34025	2215	-1.30551	2216	-0.48011	1
2217	0.27134	2218	1.12519	2219	1.83113	2220	2.59681	1
2221	3.39403	2222	3.84895	2223	4.02233	2224	3.93750	1
2225	3.64622	2226	3.20813	2227	2.59681	2228	3.39403	1
2229	3.84895	2230	4.02233	2231	3.93750	2232	3.64622	1
2233	3.20813	2239	-3.39403	2240	-3.84895	2241	-4.02233	1
2242	-3.93750	2243	-3.64622	2244	-2.59681	2245	-3.39403	1
2246	-3.84895	2247	-4.02233	2248	-3.93750	2249	-3.64622	1
23 8	56.8554	23 9	56.8736	2310	56.8844	2311	56.8827	1
2312	56.8702	2313	56.8367	2314	-56.8367	2315	-56.8702	1
2316	-56.8827	2317	-56.8844	2318	-56.8736	2319	-56.8554	1
2320	0.0	2321	-15.8462	2322	-31.8510	2323	-47.9019	1
2324	-63.5718	2325	-78.4498	2326	-92.3667	2327	0.0	1
2328	15.8462	2329	31.8510	2330	47.9019	2331	63.5718	1
2332	78.4498	2333	92.3667	2339	-15.8462	2340	-31.8510	1
2341	-47.9019	2342	-63.5718	2343	-78.4498	2344	0.0	1
2345	15.8462	2346	31.8510	2347	47.9019	2348	63.5718	1
2349	78.4498	2412	6.8182	2511	7.4397	2610	7.6599	1
27 9	7.5385	28 8	1.0	29 1	1.0	29 2	1.0	1
29 3	1.0	29 4	1.0	29 5	1.0	29 6	1.0	1
29 7	1.0	29 8	0.03219	29 9	0.01978	2910	0.00477	1
2911	-0.00844	2912	-0.02295	2913	-0.04114	2914	-0.04114	1
2915	-0.02295	2916	-0.00844	2917	0.00477	2918	0.01978	1
2919	0.03219	2920	0.01009	2921	0.01415	2922	0.01555	1
2923	0.01487	2924	0.01249	2925	0.00971	2926	0.00705	1
2927	0.01009	2928	0.01415	2929	0.01555	2930	0.01487	1
2931	0.01249	2932	0.00971	2933	0.00705	2934	-0.76286	1
2935	-0.77019	2936	-0.78969	2937	-0.81957	2938	-0.84856	1
2939	-0.01415	2940	-0.01555	2941	-0.01487	2942	-0.01249	1
2943	-0.00971	2944	-0.01009	2945	-0.01415	2946	-0.01555	1
2947	-0.01487	2948	-0.01249	2949	-0.00971	30 9	1.0	1
3018	-1.0	3119	1.0	3117	-1.0	3211	1.0	1
3216	-1.0	3312	1.0	3315	-1.0			2

TABLE VI

MATRIX F INPUT FORM

1 1	40.5860	2 2	4712.54	2 9	568.242	229	656.335	1
221	-334.075	244	-289.5395	3 3	36.7518	4 4	35.4129	1
5 5	36.0195	6 6	37.5382	7 7	41.9716	8 8	1554.5632	1
814	-395.2744	815	-438.193	822	-109.0759	823	-121.1411	1
9 9	418.3898	910	-123.270	934	-335.6280	944	-70.3038	1
945	63.0954	1010	272.7594	1011	-90.9668	1034	236.8452	1
1035	-207.059	1045	-38.5243	1046	42.6268	1111	209.5613	1
1112	-79.0163	1135	150.650	1136	-162.1008	1146	-27.5895	1
1147	34.1926	1212	194.0944	1213	-80.2663	1236	123.1598	1
1237	-156.6048	1247	-23.5277	1248	31.7581	1313	199.3646	1
1314	-85.8209	1337	124.342	1338	-169.2272	1348	-23.198	1
1349	31.517	1414	327.7679	1422	64.8044	1438	137.6857	1
1449	-23.8269	1515	372.3846	1516	-102.9527	1523	72.1931	1
1538	165.0686	1543	-28.6228	1616	239.4731	1617	-97.174	1
1637	150.4141	1638	-22.5909	1642	-28.2054	1643	37.8843	1
1717	236.6195	1718	-96.6455	1736	150.466	1737	-189.7857	1
1741	-28.9633	1742	38.8136	1818	259.1003	1819	-113.6383	1
1835	188.301	1836	-198.8093	1840	-34.6218	1841	42.5174	1
1919	332.4463	1920	-146.3721	1934	280.9922	1935	-259.2942	1
1939	-45.7466	1940	53.9308	2020	489.4772	2021	-81.2121	1
2034	-389.6962	2039	75.1214	2121	68.9996	2222	23.2739	1
2323	26.1248	2424	2.4861	2425	0.5188	2525	1.9818	1
2526	0.4721	2626	1.7829	2627	0.4193	2727	1.6776	1
2728	0.4194	2828	1.6758	2929	1.9267	2930	0.4860	1
3030	2.0048	3031	0.5164	3131	2.062	3132	0.5146	1
3232	2.0661	3233	0.5184	3333	2.7071	3434	1997.6131	1
3439	-133.6859	3445	-112.4532	3535	1194.6992	3540	-83.7719	1
3546	-66.4386	3636	822.3501	3641	-62.6632	3647	-50.6107	1
3737	808.2336	3742	-57.4131	3748	-47.0957	3838	804.7401	1
3843	-58.4006	3849	-48.6683	3939	35.7044	4040	24.5276	1
4141	18.6781	4242	14.6663	4343	14.3406	4444	59.7284	1
4545	29.7345	4646	20.3833	4747	13.0860	4848	12.6318	1
4949	11.8292							2

TABLE VII

MATRIX P

Input Form

1	1500.00	1
2	252,80	1
3	714.00	1
4	528.00	1
5	109.00	1
6	-210.50	1
7	-2782.00	1
8	-4523.56	1
9	-5212.17	1
10	-5568.74	1
11	-5395.86	1
12	-4593.58	1
13	-4654.94	1
14	-4654.94	1
15	-4593.58	1
16	-5395.86	1
17	-5568.74	1
18	-5212.17	1
19	-4523.56	1
20	2390.73	1
21	4825.58	1
22	5395.02	1
23	6125.17	1
24	6229.25	1
25	5802.52	1
26	2738.27	1
27	2390.73	1
28	4825.58	1
29	5395.02	1
30	6125.17	1
31	6229.25	1
32	5802.52	1
33	2738.27	2

TABLE VIII

EXPERIMENTAL RESULTS AT $Y_w = 34.5$

PANEL NO.	GAGE NO.		STRAIN READINGS		AVERAGE STRAINS	σ max / σ min	τ max
	Interior	Exterior	Interior	Exterior			
15		486		61	61	1094.02	
		485		118	118		1008.22
		484		-50	-50	-922.41	
21	279	459	17	25	21	851.68	
	280	458	95	100	97.5		726.87
	281	457	04	-14	-5	-602.06	
25	367	468	16	-43	-13.5	678.15	
	368	467	-47	-99	-73		627.44
	369	466	29	11	20	-576.74	
28	28	474	-19	34	7.5	960.47	
	29	473	137	86	111.5		827.86
	30	472	27	-8	9.5	-695.25	
30	89	477	9	9	9	457.66	
	90	476	55	63	59		512.27
	91	475	-12	-20	-16	-566.87	
34	19	480	-10	-21	-15.5	599.43	
	20	479	76	65	70.5		568.22
	21	478	29	10	19.5	-537.02	
38	13	483	-80	-76	-78	495.37	
	14	482	61	62	61.5		803.49
	15	481	35	42	38.5	-1111.62	

TABLE IX

Comparison of Results at Station Y_w = 34.5. Loading 336,000 in. lbs. of torque. Principal axis is measured from load reference axis, the Center Intermediate Beam, which has 33° 58' sweep back.

PANEL NO.	MAX. or MIN. NORMAL STRESS		MAXIMUM SHEAR STRESS		PRINCIPAL AXIS	
	Experimental	Theoretical	Experimental	Theoretical	Experimental	Theoretical
15	1094.02	1605.47	1008.22	1333.88	31° 52'	30° 12'
17		1530.10		1092.17		28° 16'
19		1047.07		895.67		38° 32'
21	851.68	678.85	726.87	845.91	40° 52'	40° 43'
23		-792.63		819.44		48° 05'
25	-602.06	-970.55	627.44	1033.12	38° 48'	49° 20'
REAR BEAM						
28	960.47	767.42	827.86	870.20	44° 44'	47° 36'
30	457.66	626.57	512.27	556.54	39° 20'	45° 24'
32		813.00		669.19		40° 12'
34	599.43	851.95	568.22	761.82	37° 26'	39° 55'
36		-767.60		901.15		35° 49'
38	-1111.62	-1052.83	803.49	1160.03	27° 11'	33° 56'

TABLE X

COMPARISON OF THEORETICAL RESULTS AT STATION Y_w = 34.5

(1) WITHOUT INCLUDING CENTER SECTION, AS IN REF. 2.

(2) INCLUDING CENTER SECTION

PANEL NO.	MAXIMUM NORMAL STRESS		MINIMUM NORMAL STRESS		MAXIMUM SHEAR STRESS	
	(1)	(2)	(1)	(2)	(1)	(2)
15	2234	1605	-1280	-1062	1757	1334
17	2025	1530	-651	-654	1338	1092
19	1420	1047	-630	-744	1025	896
21	1009	679	-679	-1013	844	846
23	827	846	-619	-793	723	819
25	994	1095	-418	-970	706	1033
28	813	973	-373	-767	593	870
30	714	626	-478	-486	596	556
32	835	813	-505	-525	670	669
34	1068	852	-478	-672	773	762
36	1575	1034	-575	-768	1075	901
38	1982	1267	-1004	-1053	1493	1160

TABLE XI

MATRIX OF ALL INTERNAL LOADS
$\{AT\} = [S]\{P\}$
FROM IDEALIZED MODEL WITH CENTER SECTION INCLUDED

1	174.54054260		
2	1325.45092773	26	266.98681641
3	462.C3833CC8	27	1781.35253906
4	474.22583CC8	28	3944.20239258
5	675.57104492	29	-84C7.73046875
6	1C66.64038086	3C	-7190.99218750
7	-597.CCC24414	31	-5754.24218750
8	-3451.C1147461	32	-4264.46093750
9	-3498.75415039	33	-2847.58496094
1C	-4256.81250CCC	34	650.99536133
11	-5356.39062500	35	716.78784180
12	-5181.C3906250	36	392.53369141
13	-4882.48437500	37	-136.54725647
14	-7350.36718750	38	1679.07592773
15	-7291.8125000C	39	6767.17968750
16	-5829.66796875	40	6785.34375000
17	-5258.51953125	41	5224.67187500
18	-4711.71093750	42	985.44262695
19	-4C13.84619141	43	10263.53515625
2C	-34C7.25048828	44	3625.59106445
21	397C.23242188	45	6134.81640625
22	2286.73657227	46	5103.66015625
23	2C93.25366211	47	3034.79296875
24	-1755.84497070	48	4810.60546875
25	-579.25122070	49	6030.46484375

TABLE XII

MATRIX OF ALL INTERNAL LOADS
{AT}=[S]{P}
FROM IDEALIZED MODEL WITH CENTER SECTION NOT INCLUDED

1	-92.32380676	26	-1100.95019531
2	1592.31518555	27	-939.57446289
3	-60.23043823	28	-859.61694336
4	-222.62962341	29	-3524.74560547
5	-253.08834839	30	-3361.27685547
6	-94.43901062	31	-3227.84252930
7	442.25463867	32	-2977.40502930
8	-2286.37548828	33	-2714.04394531
9	-3785.30151367	34	767.79956055
10	-4119.09765625	35	904.96679687
11	-4763.98437500	36	592.91650391
12	-4985.19921875	37	-17.30769348
13	-4969.66796875	38	-720.50903320
14	-4492.27343750	39	8591.92187500
15	-4354.52343750	40	8726.14062500
16	-4886.99609375	41	7870.36718750
17	-5013.01953125	42	4969.57031250
18	-4765.91015625	43	1010.43847656
19	-4219.25390625	44	5460.73437500
20	-3867.24985352	45	8681.62500000
21	5143.68750000	46	8357.03125000
22	200.63256836	47	7980.82031250
23	-379.16625977	48	4503.76171875
24	-1720.40966797	49	769.41943359
25	-1354.33056641		

REFERENCES

1. Wehle, L. B., Jr., and W. Lansing. "A method for Reducing the Analysis of Complex Redundant Structures to a Routine Procedure," Journal of the Aeronautical Sciences, pp. 677-684, October 1952

2. Holgren, M. A., and C. L. Comfort. "Comparison of Experimental Stresses and Deflections with Those Predicted by a Strain Energy Method for an F8U-3 Wing Loaded in Torsion." Unpublished Master's thesis, Naval Postgraduate School, Monterey, California, 1963.

3. Smith, C. F. "Stress and Deflection Analysis of Aircraft Structures Using Strain Energy Theory in Conjunction with Electronic Digital Computers," Report 10917. Dallas, Texas: Chance Vought Aircraft, Inc., November 1957.

4. Bruhn, E. F., and A. F. Schmitt. Analysis and Design of Aircraft Structures, Vol. 1, Chapter A7. Cincinnati, Ohio: Tri-State Offset Company, 1965.

5. Lang, A. L., and R. L. Bisplinghoff. "Some Results of Swept-back Wing Structural Studies," Journal of the Aeronautical Sciences, Vol. 18, No. 11, pp. 705-717, November 1951.

6. Garvey, S. J. "The Quadrilaterial Shear Panel," Aircraft Engineering, Vol. 23, pp. 134-144, May 1951.

7. Eggertz, S. "Calculation of Stresses in a Swept Multicell Cantilever Box Beam with Ribs Perpendicular to the Spars and Comparison of Results," Report 54. FLGTEKNISKA FORSOKSANSTALTEN, the Aeronautical Research Institute of Sweden, Stockholm, March 1954.

APPENDIX A

PROGRAM ENERGY

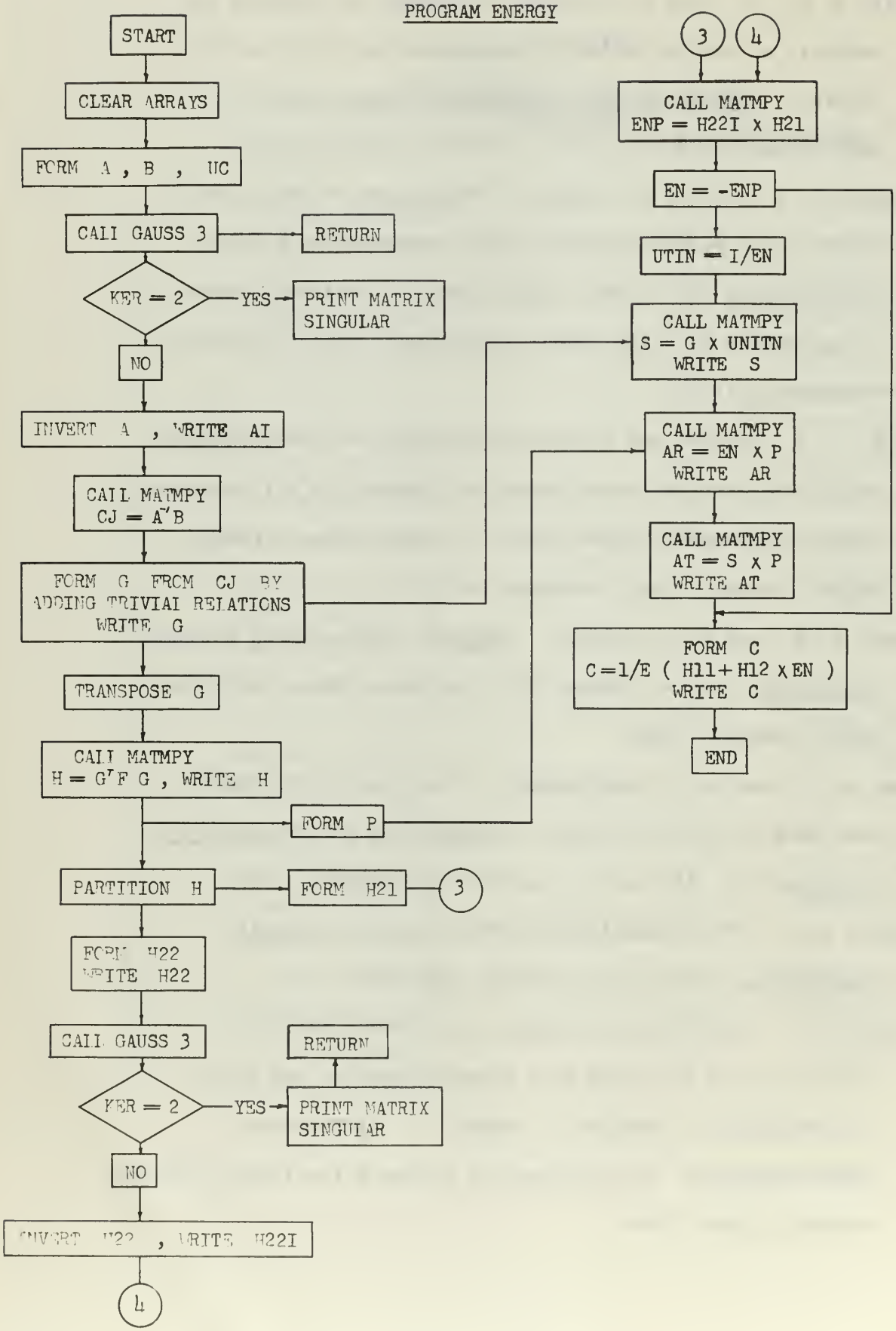

```
//ENERGY JOB  ASZ5,01FP,5,5 , MESSERSCHMIDT,D.B. ,MSGLEVEL 1
//      EXEC FORTCLG
//FORT.SYSIN DD *
C       COEFFICIENT MATRICES A, B, AND UC ARE BASIC STRUCTURAL DATA
      0DIMENSION A(50,50),AI(50,50),B(50,50),CJ(50,50),UC(50,50),
      1G(50,50),H(50,50),GT(50,50),H22(50,50),H12(50,50),UCG(50,50),
      2H21(50,50),H22I(50,50),EN(16,33),AR(16),UNITN(50,50),S(50,50),
      3AT(50),H12N(50,50),C(50,50),LIST(50),P(35),ENP(16,33)
      0EQUIVALENCE(A,CJ,UCG,H22,H21,S),(B,G,H12,C),(UC,H),
      1(AI,GT,H22I,UNITN,H12N)
C       CLEAR ARRAYS TO RECEIVE INPUT
        DO 10 I=1,50
        DO 10 J=1,50
        A(I,J) = 0.0
        B(I,J) = 0.0
        UC(I,J) = 0.0
   10   AI(I,J) = 0.0
C       READ NON REDUNDANT MATRIX A
   31   CALL INPUT(50,A)
        GO TO (31,32),NEXT
C       READ LOAD AND REDUNDANT MATRIX B
   32   CALL INPUT(50,B)
        GO TO (32,33),NEXT
C       FORM ENERGY COEFFICIENT MATRIX UC
   33   CALL INPUT(50,UC)
        GO TO (33,35),NEXT
   35   DO 36 I = 1,49
        DO 36 J = 1,49
   36   UC(J,I) = UC(I,J)
C       INVERT THE A MATRIX
        CALL GAUSS3(33,1.E-10,A,AI,KER)
        GO TO(365,364),KER
  364   PRINT 151
  151   FORMAT(24H     MATRIX A IS SINGULAR)
  365   PRINT 200
   37   PRINT 38
   380FORMAT(64H A MATRIX INVERSE BY GAUSS3, 9 COLUMNS, IE 1'9, 10 18...
     1PER PAGE//
        PRINT 100,((AI(I,J),J=1,9),I=1,33)
        PRINT 200
        PRINT 100,((AI(I,J),J=10,18),I=1,33)
        PRINT 200
        PRINT 100,((AI(I,J),J=19,27),I=1,33)
        PRINT 200
        PRINT 300,((AI(I,J),J=28,33),I=1,33)
  100   FORMAT(/9F10.6)
  150   FORMAT(/11F10.6)
  200   FORMAT(1H1)
C       POST MULTIPLY AI WITH B MATRIX
        CALL MATMPY(33,33,49,AI,B,CJ)
C       FORM G MATRIX BY ADDITION OF TRIVIAL RELATIONS TO CJ
        DO 40 I=34,49
   40   CJ(I,I) = 1.0
        DO 41 I=1,49
        DO 41 J=1,49
   41   G(I,J) = CJ(I,J)
        PRINT 200
   42   PRINT 43
   43   FORMAT(50H  G MATRIX ,FORMED FROM CJ WITH TRIVIAL RELATIONS//)
        PRINT 100,((G(I,J),J=1,9),I=1,49)
        PRINT 200
        PRINT 100,((G(I,J),J=10,18),I=1,49)
        PRINT 200
        PRINT 100,((G(I,J),J=19,27),I=1,49)
        PRINT 200
        PRINT 100,((G(I,J),J=28,36),I=1,49)
        PRINT 200
        PRINT100,((G(I,J),J=37,45),I=1,49)
        PRINT 200
        PRINT 400,((G(I,J),J=46,49),I=1,49)
  300   FORMAT (/ 6F13.7)
  400   FORMAT (/ 4F13.7)
C       TRANSPOSE G
        DO 44 I=1,49
        DO 44 J=1,49
   44   GT(I,J) = G(J,I)
C       FORM H MATRIX BY TRIPLE PRODUCT (GT)(UC)(G)
        CALL MATMPY(49,49,49,UC,G,UCG)
        CALL MATMPY(49,49,49,GT,UCG,H)
        PRINT 200
        PRINT 45
```

```
   45 FORMAT(44H MATRIX H FORMED BY TRIPLE  PRODUCT, GTXUCXG//)
      PRINT 500,((H(I,J),J=1,9),I=1,49)
      PRINT 200
      PRINT 500,((H(I,J),J=10,18),I=1,49)
      PRINT 200
      PRINT 500,((H(I,J),J=19,27),I=1,49)
      PRINT 200
      PRINT 500,((H(I,J),J=28,36),I=1,49)
      PRINT 200
      PRINT 500,((H(I,J),J=37,45),I=1,49)
      PRINT 200
      PRINT 600,((H(I,J),J=46,49),I=1,49)
  500 FORMAT (/9F13.4)
  600 FORMAT (/ 4F13.4)
C     READ LOAD MATRIX  P
      DO 510 I = 1,35
  510 P(I) = 0.0
   57 READ(5,58) I, (P(I)),NEXT
   58 FORMAT (I2  , F12.4, I1 )
      GO TO (57,581),NEXT
C     PARTITION  H MATRIX
  581 DO 54  I=34,49
      DO 54  J=34,49
      II = I-33
      JJ = J-33
   54 H22(II,JJ) = H(I,J)
      PRINT 200
  521 PRINT 522,((H22(I,J),J = 1,8),I = 1,16 )
  522 FORMAT(/8F12.4)
      PRINT 200
      PRINT 522,((H22(I,J),J = 9,16),I = 1,16)
C     INVERT  H22 MATRIX
      CALL GAUSS 3 (16,1.E-10, H22, H22I,KER)
      GO TO(525,524),KER
  524 PRINT 150
      PRINT 200
  525 PRINT 522,((H22I(I,J),J=1,8),I=1,16)
      PRINT 522,((H22I(I,J),J=9,16),I=1,16)
      DO 53 I = 34,49
      DO 53  J=1,33
      KK = I-33
   53 H21(KK,J)  H(I,J)
C     FORM REDUNDANT LOAD COEFFICIENT MATRIX, EN.
      DO 540 I=1,16
      DO 540 K=1,33
      SUM = 0.0
      DO 541 J=1,16
  541 SUM = SUM + H22I(I,J)*H21(J,K)
  540 ENP(I,K) = SUM
      DO 56  I=1,16
      DO 56  J=1,33
   56 EN(I,J) = -1.0 * ENP(I,J)
C     FORM MATRIX  UNITN BY PLACING EN  BELOW  UNIT MATRIX
      DO 99 I = 1,33
      DO 99 J = 1,33
   99 UNITN(I,J) = 0.0
      DO 62  I = 1,33
   62 UNITN(I,I) = 1.0
      DO 63  I=34,49
      DO 63  J=1,33
      KK = I-33
   63 UNITN(I,J) = EN(KK,J)
C     FORM S MATRIX .  S = (G)(UNITN)
      CALL MATMPY (49,49,33, G, UNITN, S )
      PRINT 200
      PRINT 800
  800 FORMAT (43H STRESS COEFFICIENT MATRIX.  S = (G)(UNITN) //)
      PRINT 150,((S(I,J),J=1,11),I = 1,49)
      PRINT 200
      PRINT150, ((S(I,J),J=12,22),I = 1,49)
      PRINT 200
      PRINT150,((S(I,J),J=23,33),I=1,49 )
C     REDUNDANT LOAD MATRIX, AR
      DO 80 I = 1,16
      SUM = 0.0
      DO 81 J = 1,33
   81 SUM = SUM + EN(I,J)*P(J)
   80 AR(I)  =  SUM
      DO 59  I=1,49
   59 LIST(I) = 3*I
      PRINT 200
```

```
      PRINT 60
  600 FORMAT (50H REDUNDANT LOAD MATRIX.  AR   -  H22I    H21    P  //
     1   16H AR(1-16)= A(   ))
      PRINT 700,(LIST(J),AR(J),J=1,16)
  700 FORMAT (/13X,I2,F20.8)
C     TOTAL UNKNOWN INTERNAL LOADS.  AT = (S)(P)
      DO 640 I=1,49
      SUM = 0.0
      DO 641 J=1,33
  641 SUM = SUM + S(I,J)*P(J)
  640 AT(I) = SUM
      PRINT 200
      PRINT 900
 9000 FORMAT ( 45H  MATRIX OF ALL INTERNAL LOADS.  AT= (S)(P)  //
     1 16H AT(I)    = A(   ) )
      PRINT 1000, (LIST(I),AT(I) , I=1,49 )
 1000 FORMAT (/13X,I2,F20.8)
      DO 52  I=1,33
      DO 52  J=34,49
   52 H12(I,J-33) = H(I,J)
      E = 10300000.0
C     INFLUENCE COEFFICIENT MATRIX.  C = ( H11 + (H12) (EN)) / E
      DO 90  I = 1,33
      DO 90  K = 1,33
      SUM = 0.0
      DO 95  J = 1,16
   95 SUM = SUM + H12(I,J)*EN(J,K)
   90 H12N(I,K) = SUM
      SCALE = 10000.
      DO 70  I=1,33
      DO 70  J=1,33
   70 C(I,J) = ((H(I,J)  +  H12N(I,J))/E)*SCALE
      PRINT 200
      PRINT 73
   730 FORMAT (45 H MATRIX OF DEFLECTION INFLUENCE COEFFICIENTS  /
     135H  C   =((H11 +(H12)(N ))/ E)*(SCALE))
      PRINT 150,((C(I,J),J= 1,11),I=1,33 )
      PRINT 200
      PRINT 150, ((C(I,J),J=12,22),I=1,33)
      PRINT 200
      PRINT 150,((C(I,J),J=23,33),I=1,33)
      RETURN
      END
      SUBROUTINE  GAUSS3(N,EP,AS,XS,KER)
      IMPLICIT REAL*8(A-H),REAL*8(O-P)
      REAL*4 AS(50,50),XS(50,50),EP
      DIMENSION(A 50,50),X(50,50)
      DO 1 I=1,N
      DO 1 J=1,N
      A(I,J)=AS(I,J)
    1 X(I,J)=0.0
      DO 2 K=1,N
    2 X(K,K)=1.0
   10 DO 34 L=1,N
      KP=0
      Z=0.0
      DO 12 K=L,N
      IF(Z-DABS(A(K,L))) 11,12,12
   11 Z=DABS A K,L
      KP=K
   12 CONTINUE
      IF(L-KP)13,20,20
   13 DO 14 J=L,N
      Z=A(L,J)
      A(L,J)=A(KP,J)
   14 A(KP,J)=Z
      DO 15 J=1,N
      Z=X(L,J)
      X(L,J)=X(KP,J)
   15 X(KP,J)=Z
   20 IF(DABS(A(L,L))-EP)50,50,30
   30 IF(L-N)31,34,34
   31 LP1=L+1
      DO 36 K=LP1,N
      IF(A(K,L)) 32,36,32
   32 RATIO=A(K,L)/A(L,L)
      DO 33 J=LP1,N
   33 A(K,J)= A(K,J)-RATIO*A(L,J)
      DO 35 J=1,N
   35 X(K,J)=X(K,J)-RATIO*X(L,J)
   36 CONTINUE
```

```
 34 CONTINUE
 40 DO 43 I=1,N
    II=N+1-I
    DO 43 J=1,M
    S=0.0
    IF(II-N)41,43,43
 41 IIP1=II+1
    DO 42 K=IIP1,N
 42 S=S+A(II,K)*X(K,J)
 43 X(II,J)=(X(II,J)-S)/A(II,II)
    KER=1
    DO 51 I=1,N
    DO 51 J=1,N
 51 XS(I,J) = X(I,J)
    RETURN
 50 KER=2
    RETURN
    END
    SUBROUTINE MATMPY (L, M, N, A, B, C)
    DIMENSION A(50,50), B(50,50), C(50,50)
    DO 10 I=1,L
    DO 10 K=1,N
    SUM = 0.0
    DO 20 J=1,M
 20 SUM = SUM + A(I,J) * B(J,K)
 10 C(I,K) = SUM
    RETURN
    END
    SUBROUTINE INPUT (N,A)
    DIMENSION A(N,N),K(6)
   1EQUIVALENCE (K(1),J1),(K(2),J2),(K(3),J3),(K(4),I1),
   1(K(5),I2),(K(6),I3)
  1 READ (5,21) I1,J1,A1, I2,J2,A2, I3,J3,A3, I4,J4,A4, NEXT
 21 FORMAT (4(2I2,F12.6),I1)
    DO 10 I=1,6
    IF (K(I) .GT. N) GO TO 100
 10 CONTINUE
    IF (I1.NE. 0) A(I1,J1) = A1
    IF (I2.NE. 0) A(I2,J2) = A2
    IF (I3.NE. 0) A(I3,J3) = A3
    IF (I4.NE. 0) A(I4,J4) = A4
    GO TO (1,2), NEXT
  2 RETURN
100 PRINT 101,K,I1,J1,A1,I2,J2,A2,I3,J3,A3,I4,J4,A4
101 FORMAT (' K=',F5/ 1X, 4(2I2,F12.6))
    STOP
    END
```

APPENDIX B
PROGRAM RECROSE

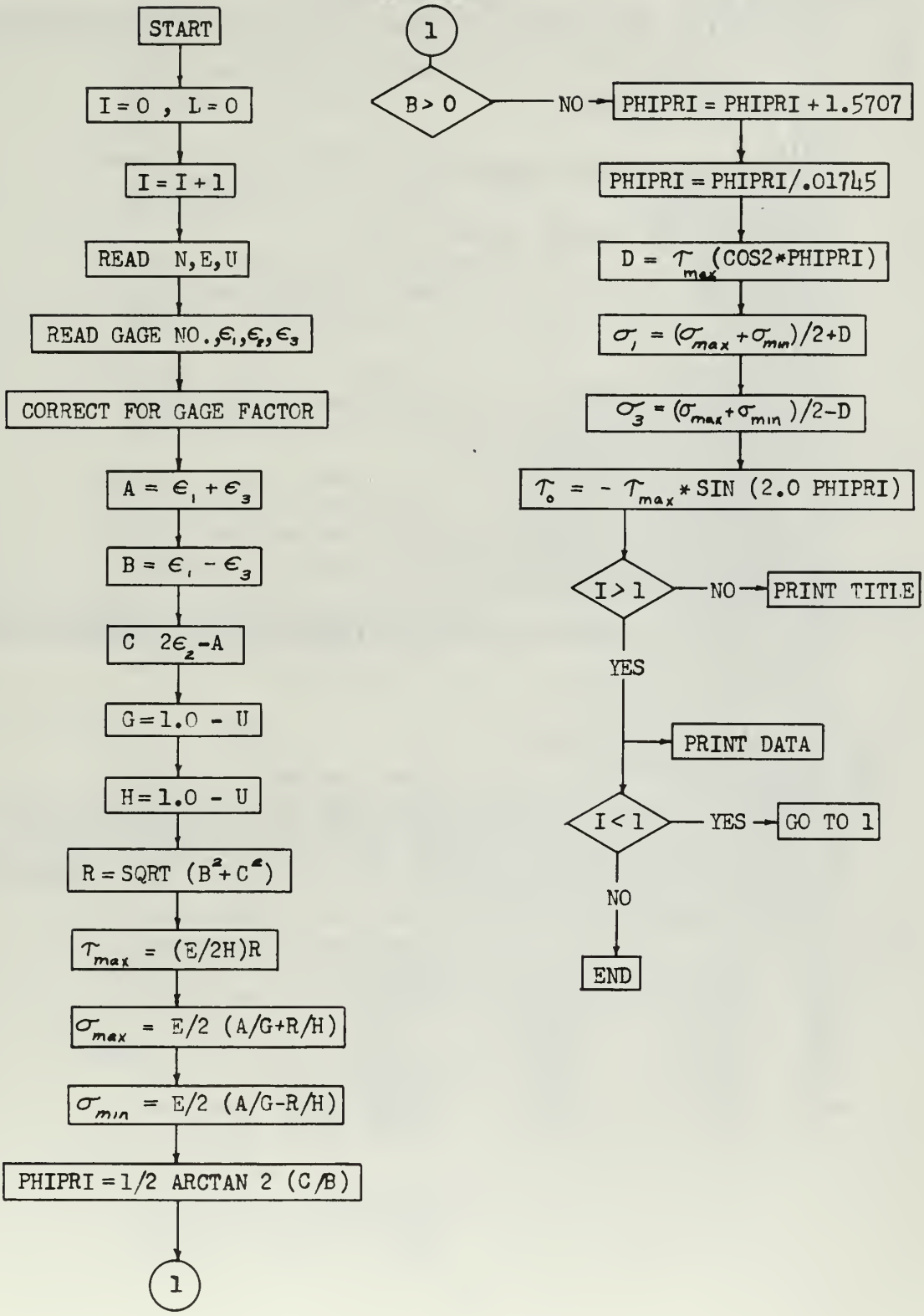

```
//RECROSE JOB  ASZ5,01FP , MESSERSCHMIDT,D.B. ,MSGLEVEL 1
// EXEC FORTCLG
//FORT.SYSIN DD *
C       RECTANGULAR STRAIN ROSETTE DATA REDUCTION FOR THE DETERMINATION
C       OF PRINCIPAL AXES, PRINCIPAL STRESSES, MAXIMUM SHEARING STRESSES,
C       AND STRESSES ALONG THE ROSETTE AXES 1 AND 3.
C
C
        READ (5,100) N,E,U
        L=0
        I=0
      1 I=I+1
        READ  5,101  IGAGE,E1,E2,E3
        E1=E1*1.0E-06
        E2=E2*1.0E-06
        E3=E3*1.0E-06
C       CORRECTION FOR A GAGE FACTOR =  1.95
        E1=E1*1.03
        E2=E2*1.03
        E3=E3*1.03
        G=1.0-U
        H=1.0+U
        A=E1+E3
        B=E1-E3
        C=(2.0*E2)-A
        R=SQRT((B**2)+(C**2))
        TAUMAX=(E/(2.0*H))*R
        SIGMAX=(E/2.0)*((A/G)+(R/H))
        SIGMIN=(E/2.0)*((A/G)-(R/H))
        PHIPRR=0.5*(ATAN2(C,B))
        IF (B.GE.0.0) GO TO 2
        PHIPRR=PHIPRR+1.5707963
      2 PHIPRD=PHIPRR/.1745329E-01
        D=TAUMAX*COS(2.0*PHIPRR)
        SIGMA1=((SIGMAX+SIGMIN)/2.0)+D
        SIGMA3=((SIGMAX+SIGMIN)/2.0)-D
        TAUO=-TAUMAX*SIN(2.0*PHIPRR)
        IF (I.GT.1) GO TO 3
        WRITE (6,102)
      3 WRITE (6,103) IGAGE,E1,SIGMAX,E2,SIGMIN,E3,TAUMAX,SIGMA1,PHIPRR,
     9SIGMA3,PHIPRD,TAUO
        L=L+11
        IF (L.LT.66) GO TO 4
        WRITE (6,102)
        L=0
      4 IF (I.LT.N) GO TO 1
    100 FORMAT (I8,E17.7,F10.5)
    101 FORMAT (I8,3F12.5)
    102 FORMAT (1H1)
    103 FORMAT (T6,'ROSETTE NUMBER',I8,//,T16,'E1=',F14.7,' IN/IN',T45,
       3'SIGMAX=',F14.7, 'PSI',/,T16,'E2=',F14.7, 'IN/IN',T45,'SIGMIN=',
       3F14.7, 'PSI',/,T16,'E3=',F14.7, 'IN/IN',T45,'TAUMAX=',F14.7,
       3 'PSI',//,T11,'SIGMA 1=',F14.7, 'PSI',T45,'PHI PR=',F14.7,' RADIAN
       3S',/,T11,'SIGMA 3=',F14.7, 'PSI',T45,'PHI PR=' ,F14.7, 'DEGREES',/,
       3T13,'TAU O=',F14.7, 'PSI',//
        RETURN
        END
/*
//GO.SYSIN DD *
        8     0.1300000E 08    0.32
       15       36.5            118.0          -13.5
       21       21.0             97.5           -5.0
       25      -13.5            -73.0           20.0
       28        7.5            111.5            9.5
       33        9.0             59.0          -16.0
       34      -15.5             70.5           19.5
       38      -78.0             61.5           38.5
      484       61.0            118.0          -50.0
/*
```

INITIAL DISTRIBUTION LIST

		NO. COPIES
1.	Defense Documentation Center Cameron Station Alexandria, Virginia 22314	20
2.	Library Naval Postgraduate School Monterey, California	2
3.	Commandant of the Marine Corps Headquarters, U.S. Marine Corps Washington, D. C. 22214	1
4.	Chairman, Department of Aeronautics Naval Postgraduate School Monterey, California	2
5.	Professor Charles H. Kahr Department of Aeronautics Naval Postgraduate School	3
6.	Professor Ulrich Haupt Department of Aeronautics Naval Postgraduate School Monterey, California	1
7.	Major Donald B. Messerschmidt 381-A Bergin Drive Monterey, California	2
8.	Dr. E. S. Lamar Chief Scientist Naval Air Systems Command Department of Navy Washington, D. C. 20360	1
9.	Mr. G. L. Desmond Aerodynamics and Structures Technology Adminstrator Department of the Navy Naval Air Systems Command Washington, D. C. 20360	1
10.	Commander Naval Air Systems Command Deaprtment of the Navy Washington, D. C. 20360	1
11.	Prof. A. E. Fuhs Department of Aeronautics Naval Postgraduate School Monterey, Calif. 93940	1

Security Classification

DOCUMENT CONTROL DATA - R&D

(Security classification of title, body of abstract and indexing annotation must be entered when the overall report is classified)

1. ORIGINATING ACTIVITY (Corporate author)	2a. REPORT SECURITY CLASSIFICATION
Naval Postgraduate School Monterey, California	Unclassified
	2b. GROUP

3. REPORT TITLE

COMPARISON OF THEORETICAL AND EXPERIMENTAL STRESSES IN AN F8U-3 AIRPLANE WING LOADED IN TORSION

4. DESCRIPTIVE NOTES *(Type of report and inclusive dates)*

5. AUTHOR(S) *(Last name, first name, initial)*

Messerschmidt, Donald B.

6. REPORT DATE	7a. TOTAL NO. OF PAGES	7b. NO. OF REFS
December 1967	66	7

8a. CONTRACT OR GRANT NO.	9a. ORIGINATOR'S REPORT NUMBER(S)
b. PROJECT NO.	
c.	9b. OTHER REPORT NO(S) *(Any other numbers that may be assigned this report)*
d.	

10. AVAILABILITY/LIMITATION NOTICES

[redacted]

11. SUPPLEMENTARY NOTES	12. SPONSORING MILITARY ACTIVITY
	Naval Postgraduate School Monterey, California

13. ABSTRACT

The stresses near the root of an F8U-3 airplane wing loaded in torsion were found using the matrix-force method of analysis. The wing was represented by a simplified, idealized model consisting of axial-load carrying flange bars and shear carrying cover plates. The theoretical stresses in the idealized model were found by using the IBM 360/67 computer to solve for the redundant loads. These stresses show favorable comparison with the experimental stresses determined from strain gages mounted on the cover skin of the wing. This study shows that the matrix-force method is applicable to thick-skinned wings.

DD FORM 1 JAN 64 1473

Security Classification

14. KEY WORDS	LINK A		LINK B		LINK C	
	ROLE	WT	ROLE	WT	ROLE	WT
Matrix-force method						
Strain energy analysis						
Swept-wing structural analysis						

thesM558
Comparsion of theoretical and ...
DUDLEY KNOX LIBRARY
3 2768 00416481 4
DUDLEY KNOX LIBRARY